ASME VVUQ 30.1-2024

Scaling Methodologies for Nuclear Power Systems Responses

AN AMERICAN NATIONAL STANDARD

The American Society of Mechanical Engineers

ASME VVUQ 30.1-2024

Scaling Methodologies for Nuclear Power Systems Responses

AN AMERICAN NATIONAL STANDARD

The American Society of Mechanical Engineers

Two Park Avenue • New York, NY • 10016 USA

Date of Issuance: June 28, 2024

This Standard will be revised when the Society approves the issuance of a new edition.

This code or standard was developed under procedures accredited as meeting the criteria for American National Standards. The standards committee that approved the code or standard was balanced to ensure that individuals from competent and concerned interests had an opportunity to participate. The proposed code or standard was made available for public review and comment, which provided an opportunity for additional public input from industry, academia, regulatory agencies, and the public-at-large.

ASME does not "approve," "certify," "rate," or "endorse" any item, construction, proprietary device, or activity. ASME does not take any position with respect to the validity of any patent rights asserted in connection with any items mentioned in this document, and does not undertake to insure anyone utilizing a standard against liability for infringement of any applicable letters patent, nor does ASME assume any such liability. Users of a code or standard are expressly advised that determination of the validity of any such patent rights, and the risk of infringement of such rights, is entirely their own responsibility.

Participation by federal agency representatives or persons affiliated with industry is not to be interpreted as government or industry endorsement of this code or standard.

ASME accepts responsibility for only those interpretations of this document issued in accordance with the established ASME procedures and policies, which precludes the issuance of interpretations by individuals.

The endnotes and preamble in this document (if any) are part of this American National Standard.

ASME Collective Membership Mark

The American Society of Mechanical Engineers
Two Park Avenue, New York, NY 10016-5990

CONTENTS

FOREWORD

The ASME Codes and Standards Committee for verification, validation, and uncertainty quantification in computational modeling and simulation (VVUQ Committee) is responsible for coordinating, promoting, and fostering the development of standards that provide procedures for verification, validation, and uncertainty quantification of computational models and simulations. One of the subcommittees of the VVUQ Committee is the VVUQ 30 Subcommittee, which is focused on verification, validation, and uncertainty quantification in computational simulation of nuclear system thermal fluids behavior. The VVUQ 30 Subcommittee's charter is to provide the practices and procedures for verification and validation of software* used to calculate nuclear system thermal fluids behavior. While a single model may have many uses, complex systems such as nuclear power plants require a collection of multiple models to be adequately represented. Thus, the focus of the VVUQ 30 Subcommittee is not on a single model, but a specific collection of coupled models (CCM).

Historically, one of the most challenging aspects of determining the credibility of the software* has been ensuring that the validation is applicable to the particular scenario in the real-world system. Many features including size, operating conditions, and a heating source from fission often make it infeasible to obtain prototypical experimental data for nuclear system thermal fluid behavior. Due to cost and safety reasons, experimental facilities are usually scaled down from the real-world plant. Thus, performing validation based on such facilities has the additional complexity (and task) of needing to ensure that the results from validation are applicable to the real-world system. ASME VVUQ 1 defines "applicability" as the relevance of the evidence from the verification, validation, and uncertainty quantification activities to support the use of the computational model for a context of use. However, this is a relativity new definition. In the nuclear industry, applicability, specifically as it relates to ensuring the experimental data is relevant with respect to the behavior of the real-world system, has been called scaling analysis. Scaling has been a major focus in the nuclear industry almost since its inception and has major ramifications in determining if the computational models used to simulate nuclear system thermal fluids behavior can be useful or useless. One of the challenges in obtaining appropriate experimental data for nuclear reactor systems is ensuring that the experiment contains the appropriate physical behavior. Such behavior is often directly impacted by pressures and temperatures, heat fluxes, local geometries (e.g., lengths, areas, volumes), and local fluid properties. However, it is impossible to perform an experiment where all factors can be maintained exactly as would be found in a real-world nuclear reactor.

This Standard, in its first edition, is intended to provide practices and procedures for scaling analysis methodologies. Future revisions will be published as necessary.

Following approval by the ASME VVUQ Standards Committee, ASME VVUQ 30.1-2024 was approved by the American National Standards Institute on June 12, 2024.

* In many other engineering communities, "software" is often used to refer to generic packages, such as commercial off-the-shelf programs, and a specific collection of coupled models used to simulate a specific system would still be considered a model. However, the term "software" is used here to mean the specific collection of couple models (CCM) in order to distinguish between the entire collection of models and a specific model (SM), providing a solution based on geometric configurations and initial and boundary conditions.

ASME VVUQ COMMITTEE
Verification, Validation, and Uncertainty Quantification in Computational Modeling and Simulation

(The following is the roster of the committee at the time of approval of this Standard.)

STANDARDS COMMITTEE OFFICERS

D. M. Moorcroft, *Chair*
J. S. Kaizer, *Vice Chair*
M. Pagano, *Secretary*

STANDARDS COMMITTEE PERSONNEL

G. Banyay, Pennsylvania State University
M. D. Benedict, U.S. Air Force Research Laboratory
J. Bischoff, Consultant
D. Cheng, Fluor Corp.
D. Datye, SIMULIA
K. Dowding, Sandia National Laboratories
L. Eca, Instituto Superior Técnico
C. J. Freitas, Southwest Research Institute, Inc.
Y. Hassan, Texas A&M University
M. Horner, ANSYS, Inc.
J. S. Kaizer, U.S. Nuclear Regulatory Commission
S. L. Kieweg, Sandia National Laboratories
B. Kolade, Fitila Technologies
S. Mahadevan, Vanderbilt University
D. M. Moorcroft, Federal Aviation Administration
M. Pagano, The American Society of Mechanical Engineers
S. Rachuri, CESMII
V. Sharma, Engineering Systems, Inc.
B. H. Thacker, Southwest Research Institute
T. M. Morrison, *Contributing Member*, Food and Drug Administration
J. Smith, *Contributing Member*, Consultant

ASME VVUQ 30 SUBCOMMITTEE — VERIFICATION, VALIDATION, AND UNCERTAINTY QUANTIFICATION IN COMPUTATIONAL SIMULATION OF NUCLEAR SYSTEM THERMAL FLUIDS BEHAVIOR

Y. Hassan, *Chair*, Texas A&M University
R. Schultz, *Vice Chair*, Consultant
M. Pagano, *Secretary*, The American Society of Mechanical Engineers
M. B. Dzodzo, Westinghouse Electric Co.
C. J. Freitas, Southwest Research Institute, Inc.
J. S. Kaizer, U.S. Nuclear Regulatory Commission
M. Kimber, Texas A&M University
A. Krueger, Consultant
E. Merzari, Pennsylvania State University
U. Rohatgi, Brookhaven National Laboratory
S. Treasure, Rolls-Royce, PLC
A. V. Lozada, Defense Nuclear Facilities Safety Board
J. Adams, *Contributing Member*, Rolls-Royce, PLC
Y. Addad, *Contributing Member*, Khalifa University
A. M. F. Alwafi, *Contributing Member*, KACST
P. Balestra, *Contributing Member,* Idaho National Laboratory
D. Datye, *Contributing Member*, SIMULIA
F. D'Auria, *Contributing Member*, Universita Degli Studi Di Pisa
M. D. DeHart, *Contributing Member*, Idaho National Laboratory
N. Dinh, *Contributing Member*, North Carolina State University — Department of Nuclear Engineering
R. B. Jackson, *Contributing Member*, Consultant
L. Lommers, *Contributing Member*, Kairos Power
K. Okamoto, *Contributing Member*, The University of Tokyo — Department of Nuclear Engineering
S. Pal, *Contributing Member*, Lawrence Livermore National Laboratory
A. Ruggles, *Contributing Member*, University of Tennessee
F. Sinan Sarikurt, *Contributing Member*, Terra Power
B. Woods, *Contributing Member*, Oregon State University
M. A. Yildiz, *Contributing Member*, X-energy
R. Zanino, *Contributing Member*, Dipartimento Energia, Politecnico Di Torino
A. Zigh, *Contributing Member*, U.S. Nuclear Regulatory Commission

CORRESPONDENCE WITH THE VVUQ COMMITTEE

General. ASME codes and standards are developed and maintained by committees with the intent to represent the consensus of concerned interests. Users of ASME codes and standards may correspond with the committees to propose revisions or cases, report errata, or request interpretations. Correspondence for this Standard should be sent to the staff secretary noted on the committee's web page, accessible at https://go.asme.org/VnVcommittee.

Revisions and Errata. The committee processes revisions to this Standard on a periodic basis to incorporate changes that appear necessary or desirable as demonstrated by the experience gained from the application of the Standard. Approved revisions will be published in the next edition of the Standard.

In addition, the committee may post errata on the committee web page. Errata become effective on the date posted. Users can register on the committee web page to receive e-mail notifications of posted errata.

This Standard is always open for comment, and the committee welcomes proposals for revisions. Such proposals should be as specific as possible, citing the paragraph number, the proposed wording, and a detailed description of the reasons for the proposal, including any pertinent background information and supporting documentation.

Cases

(a) The most common applications for cases are

(1) to permit early implementation of a revision based on an urgent need

(2) to provide alternative requirements

(3) to allow users to gain experience with alternative or potential additional requirements prior to incorporation directly into the Standard

(4) to permit the use of a new material or process

(b) Users are cautioned that not all jurisdictions or owners automatically accept cases. Cases are not to be considered as approving, recommending, certifying, or endorsing any proprietary or specific design, or as limiting in any way the freedom of manufacturers, constructors, or owners to choose any method of design or any form of construction that conforms to the Standard.

(c) A proposed case shall be written as a question and reply in the same format as existing cases. The proposal shall also include the following information:

(1) a statement of need and background information

(2) the urgency of the case (e.g., the case concerns a project that is underway or imminent)

(3) the Standard and the paragraph, figure, or table number

(4) the editions of the Standard to which the proposed case applies

(d) A case is effective for use when the public review process has been completed and it is approved by the cognizant supervisory board. Approved cases are posted on the committee web page.

Interpretations. Upon request, the committee will issue an interpretation of any requirement of this Standard. An interpretation can be issued only in response to a request submitted through the online Inquiry Submittal Form at https://go.asme.org/InterpretationRequest. Upon submitting the form, the inquirer will receive an automatic e-mail confirming receipt.

ASME does not act as a consultant for specific engineering problems or for the general application or understanding of the Standard requirements. If, based on the information submitted, it is the opinion of the committee that the inquirer should seek assistance, the request will be returned with the recommendation that such assistance be obtained. Inquirers can track the status of their requests at https://go.asme.org/Interpretations.

ASME procedures provide for reconsideration of any interpretation when or if additional information that might affect an interpretation is available. Further, persons aggrieved by an interpretation may appeal to the cognizant ASME committee or subcommittee. ASME does not "approve," "certify," "rate," or "endorse" any item, construction, proprietary device, or activity.

Interpretations are published in the ASME Interpretations Database at https://go.asme.org/Interpretations as they are issued.

Committee Meetings. The VVUQ Standards Committee regularly holds meetings that are open to the public. Persons wishing to attend any meeting should contact the secretary of the committee. Information on future committee meetings can be found on the committee web page at https://go.asme.org/VnVcommittee.

SCALING METHODOLOGIES FOR NUCLEAR POWER SYSTEMS RESPONSES

1 PURPOSE, SCOPE, INTRODUCTION, AND NOMENCLATURE

1.1 Purpose

When determining the credibility of a model, a key question is what the accuracy of the computational model is for the real-world conditions where the system will operate. This accuracy is called predicative capability and is often based on the model validation. To estimate the model's predictive capability, first the error of the model needs to be determined under conditions where empirical data is available. This is referred to as the validation error. Often, based on the similarity of the test facilities and real-world systems, the validation error is used as an estimate of the model's error when making predictions on the real-world system. Thus, a key assumption is that the model's predictive capability of the real-world system is similar to the model's accuracy in predicting the empirical (experimental) data. If both systems have similar physical behavior, it is expected that the model's accuracy will be similar in both systems (the real-world system and the experiment).

There can be many reasons why the model's validation error may be very different from the model's predictive capability. While experimentalists strive to ensure that the experiment is similar to the real-world system, some sacrifices often need to be made. For example, due to the large size and inherent complexity, experimental facilities used to provide data to validate models for nuclear power plant scenarios often must be scaled down from the true nuclear power plant dimensions and operational conditions (such as pressure, temperature, and flow rates). This may include operating the experiment at lower powers and pressures, at a reduced size, or using other fluid. While these changes may not directly impact the model validation (since validation is based on the comparison of the empirical data to the model's predictions), these changes certainly impact the applicability of the model for the real-world system. For example, if a specific system was influenced by behavior that was sensitive to a characteristic length (e.g., hydraulic diameter), area (e.g., flow area), and volume, the scaled system (e.g., experiment) could not be scaled in all three values at once. Consider liquid flow through a tube. If the diameter is reduced by a factor of 2, the flow cross-section area and volume must be reduced by a factor of 4 while the wall heat transfer area is still decreased (as diameter) by a factor of 2. Thus, a phenomenon such as boiling, in which all of these geometry factors could be important, requires a method to determine if the scaled system can provide useful data, or if the scaled system is not similar to the particular scenario in the real-world system. In nuclear thermal fluid systems, the relevance of the empirical (experimental) data to the real-world system is determined through scaling analysis. Scaling is not focused on how well the computational model predicts the empirical data (i.e., validation). Instead, scaling is focused on if a model validated with the empirical data will be relevant to the real-world system. In other words, scaling formalizes the connection between the test facility and real-world system.

This Standard provides practices and procedures for determining if experimental data (used to validate models) is applicable to the real-world system. Historically, such analysis has been unique for nuclear reactor applications where conditions of fluid, both single- and two-phase, are highly size dependent due to surface-to-volume ratio, size-dependent interfacial shape (flow regimes), and interfacial area density. However, it is hoped that the presented scaling analyses methodologies developed for the nuclear community can be used to benefit other fields of engineering and science or combined with other methodologies already developed.

1.2 Scope

This Standard is focused on the scaling analysis that is used to evaluate the effects of differences (e.g., distortions) in the phenomenological behavior of experimental facilities compared to the phenomenological behavior of the real-world system. This includes scaling analysis methodologies for supporting the design of facilities and experiments capable of generating data that characterize the phenomena present in an entire system [such facilities are known as integral effects test (IET) facilities] and in components of the system (e.g., the nuclear core or the steam generator) [such facilities are known as separate effects test (SET) facilities].

Figure 1.3-1
Determination of Model Adequacy

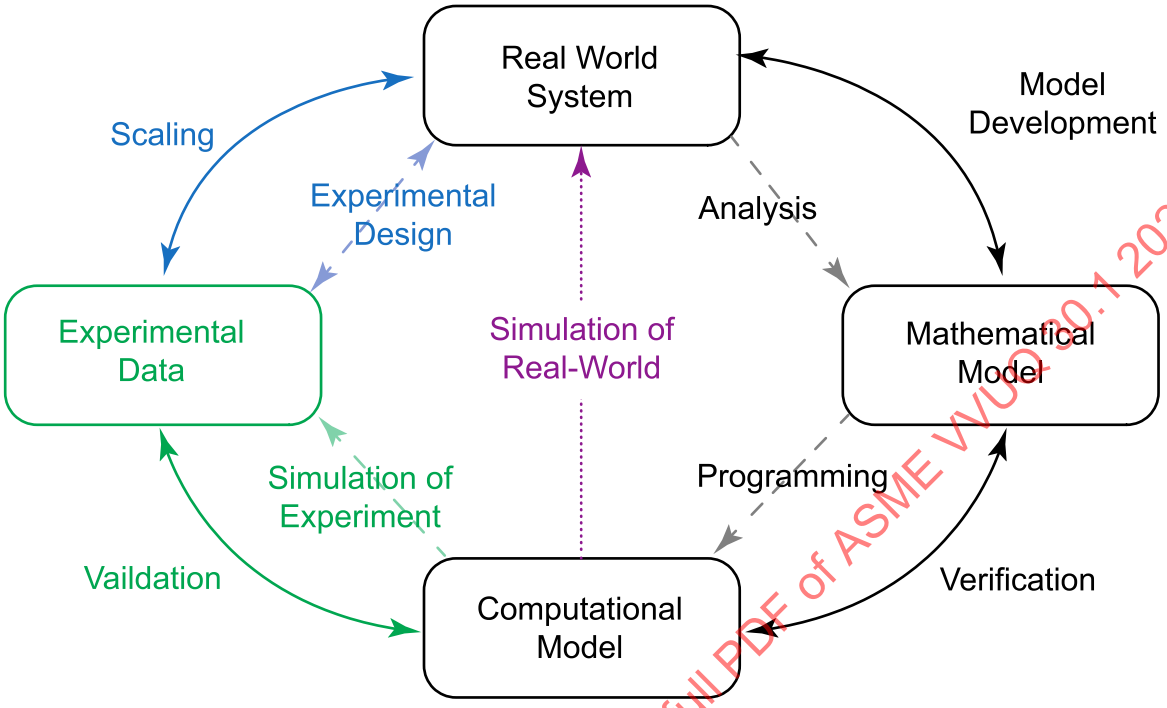

Although this best-practice Standard is focused on nuclear system applications, many portions of the methods and techniques discussed here can be applied to other engineering systems such as in chemical processing, oil and gas production, and power generation systems based on other fuel sources.

1.3 Introduction

In general, validation is the process of determining the degree to which a model represents the empirical data from the perspective of the context of model use. For nuclear reactor systems, validation is the process by which the simulation results from software (i.e., a collection of coupled models) are compared to empirical data. Generally, validation is performed to determine if the software can be used to ensure the reactor remains safe, even under accident conditions. While there are many challenges with such an analysis, one of the biggest concerns is that the system in which the experimental data is obtained is different from the real-world nuclear reactor. Thus, validation alone cannot ensure the software adequately simulates the physics of the real-world system. Additionally, the similarity of the test facility and real-world system must be assessed. This assessment must include the degree to which the developed software results can provide an adequate representation of the particular scenario in the real-world system. This requires the following additional assessments, which are independent of one another:

(a) Perform scaling analysis by assessing the relevance of the empirical data to the real-world system.

(b) Perform validation analysis by assessing the computational model's capability to predict empirical data.

Figure 1.3-1 is a modification of the classic figure by Schlesinger et al. (1979) and provides the clear distinction between the experimental data, which is used in the validation process (see green lines in Figure 1.3-1), and the real-world system. The gap between the experimental data and real-world system was recognized early in the nuclear industry, as there might be major differences in behavior between these two systems. This Standard focuses on the scaling activity (see blue lines in Figure 1.3-1) that connects experimental data to the real-world system.

Validation quantifies the error in the computational model's simulation of the experiment (see dotted green line in Figure 1.3-1). However, attention is required on the error in the computational model's simulation of the real-world system (see dotted purple line in Figure 1.3-1). Therefore, scaling is focused on ensuring that there is similarity in the behavior between the experiment and the real-world system such that the model's error from validation can be, based on the similarity, used as a reasonable estimate for the model's error in predicting the real-world system. Therefore, a scaling analysis must be performed to ensure that the model is adequate for its intended purpose.

Scaling analyses can be thought of as a quantitative way to estimate the distortion of a test facility from a real-world system. Scaling analysis started as an application of dimensional analysis and was followed by more complex analyses based on the control volume and detailed coupled-physics modeling approaches. The more complex analysis compares the phenomena that are most important in the real-world system, usually categorized by a Phenomena Identification and Ranking Table (PIRT) (Regulatory Guide 1.203, 2005). The value of the variables associated with each important phenomena from the experiment and from the real-world system are compared to ensure that either those variables have the same values (e.g., dimensionless parameters like Reynolds numbers) or that the difference in the values would not cause differences in physics (e.g., would a change in the flow area cause a different flow regime?).

By its nature, scaling analysis requires a detailed understanding of the real-world system and experimental facility. The phenomena of these systems and their interactions need to be well understood to rank the phenomena in PIRT, associate variables with the phenomena, and ensure those variables have consistent values in the experiment. However, the understanding of those phenomena and their interactions is sometimes expressed as mathematical models. Consequently, those same mathematical models are used to generate the complex computational models that need to be validated. Thus, unlike validation, which is an independent method that can be used to determine how well our models capture the physics of an experiment related to one phenomenon, some portions of scaling are sometimes dependent on the applied complex mathematical models. An incorrect understanding, expressed as an applied complex mathematical model, may be revealed through high errors when performing validation. However, an incorrect understanding, expressed as an applied complex mathematical model, could go unnoticed when performing scaling. Thus, a hierarchical approach where each phenomenon in each component and process, or interaction between two phenomena, can be separately analyzed first without the application of complex mathematical models is a necessary part of scaling analysis.

For nuclear power plants (NPPs), experiments often span a broad range of types and scopes. Some experiments are designed not to understand a component in the NPP, but a specific phenomenon. Such experiments are commonly called phenomenological tests (PTs). These experiments are typically at smaller scales and while they are primarily used to focus on a single phenomenon, they may be used to study the interactions of a few phenomena while in steady state or during transient time sequences. If the experiment is designed to only study a single phenomenon (either to understand its general behavior or its behavior in a plant component), these experiments are called SETs, as the goal of such experiments is to separate out a single effect and measures its behavior. SETs are commonly used for both model development (e.g., to generate data-driven models) and model validation because it is often possible to build these experiments much closer to the scale of the real-world system.

There is no clear distinction on when an experiment contains too many phenomena to no longer be considered a SET. However, when an experiment is meant to capture the behavior of many interacting phenomena (e.g., many components of the NPP up to and including the complete NPP), those experiments are called IETs, as the experiments attempt to best replicate the coupled behavior of the real-world system. While very useful for validation, IETs tend to be very expensive and not as versatile as SETs as their data typically cannot be used to generate data-driven models. Further, IETs may have interacting phenomena with compensating error which could result in empirical data that may not represent the real-world system. Therefore, the validation and assessment of CCM adequacy used to predict the behavior of a NPP often requires a mix of data from several SETs and IETs designed with several different scaling factors.

1.4 Nomenclature

1.4.1 Symbols

Symbol	Definition
A	Area, m^2
C	Normalized thermal resistance (Catton et al., 1990) in Nonmandatory Appendix A, section A-5
C_k	Constituents in Figure 4-1
c_p	Isobaric specific heat, J/kg K
c_v	Isochoric specific heat, J/kg K
D	Distortion, ratio of model (test facility) and prototype (plant) time ratios Π_M/Π_P, or ratio fractional changes Ω_M/Ω_P
D_p	Pipe diameter, m
E	Energy field in Figure 4-1, energy, J
e	Energy, J/kg
F	Force, N
F_k	Fields in Figure 4-1
f	Fluid, liquid phase in Figure 4-1

Table continued

Symbol	Definition
f	Decay heat fraction in Nonmandatory Appendix A, section A-5
$\overline{f}$	Time average decay heat fraction, eq. (A-5-3)
G_k	Geometrical configuration in Figure 4-1
g	Gas phase in Figure 4-1
H	Height of model or prototype, m
h	Enthalpy, J/kg
h_c	Convection heat transfer coefficient, W/m^2
h_{fg}	Difference of enthalpies, J/kg
j	General flux, shear stress, N/m^2, in eq. (A-1-4), or heat flux, W/m^2, in eq. (A-1-6)
K_s	Compliance — isentropic compressibility, m^2/N
k	Thermal conductivity, W/m K
κ	Isothermal compressibility, m^2/N
κ_S	Isentropic compressibility, m^2/N
$\overline{K}_{pin}$	Pin aggregate thermal conductivity, W/m K, eq. (A-5-19) (Catton et al., 1990)
L	Length, m
M	Mass field in Figure 4-1
M_k	Modules in Figure 4-1
MM	Momentum field in Figure 4-1
m	Mass, kg
mv	Momentum, kg m/s
$\dot{m}$	Mass flow rate, kg/s
P	Phases in Figure 4-1
P	Power, W
P_k	Processes in Figure 4-1
p	Pressure, N/m^2
q'	Decay heat, W/m
q''	Heat flux, W/m^2
$\dot{Q}$	Heat transfer rate, W
R	Pipe radius, m
Re	Reynolds number
r	Radial direction, m
S	System in Figure 4-1
S	Source terms in eqs. (5-3-1) and (5-3-2)
SS_k	Subsystem in Figure 4-1
s	Solid phase in Figure 4-1
T	Temperature, K
T_b	Bulk temperature, K
T_s	Surface temperature, K
t	Time, s
t^*	Time of peak cladding temperature, s
V	Volume, m^3
V_{CV}	Control volume, m^3
$\vec{v}$	Velocity, m/s
v	Velocity, m/s
$\overline{v}$	Average velocity, m/s
v_{fg}	Difference of specific volumes, m^3/kg
$\dot{V}$	Volumetric flow rate, m^3/s
x	Direction, m
α	Void fraction, volumetric concentration (in Figure 4-1)

Table continued

Symbol	Definition
β	Thermal expansion coefficient, 1/K
γ	Ratio of specific heats, c_p/c_v
δ	Small change
Δ	Difference
Δt	Time interval of one second, s
θ	Dimensionless temperature
$\langle\theta\rangle$	Dimensionless excess pin average temperature
ξ	Pin circumference
ϕ	Agent of change
ν	Kinematic viscosity, m^2/s
Π	Time ratios in H2TS
Π_{Bi}	Pin aggregate Biot number, eq. (A-5-19)
ρ	Density, kg/m^3
ρc	Volumetric heat capacity, J/m^3K
σ	Shear strees, N/m^2
τ	Residence time, s
Σ	Summation
ψ	State variable per unit of volume, $/m^3$
Ψ	State variable
Ψ_α	Multiplier used in eqs. (A-4-1), (A-4-2), (A-4-4) and in Table A-2-1, see eq. (A-4-3)
ω	Frequency or fractional rate of change, 1/s
$\overline{\omega}$	Effective fractional rate of change, 1/s
Ω	Fractional change (effect metrics)

1.4.2 Subscripts and Superscripts

Subscript or Superscript	Definition
A_T	Transfer area surface effects
ADS	Automatic depressurization system
b	Bulk
bk	Break
c	Cladding
CV	Control volume
D	Decay heat
d	After scram
f	Liquid phase in Figure 4-1
f	Fuel in Nonmandatory Appendix A, section A-5
fg	Fluid (liquid) and gas
g	Gas, vapor
i	Index of constituent in eqs. (5-3-1) and (5-3-2)
in	Into the control volume in Figure 5.2-1
int	Interface in Figure 5.2-1
j	Index of summation
k	Index of other interacting constituents in eqs. (5-3-1) and (5-3-2)
k	Index of phase in Nonmandatory Appendix A, section A-3
l	Liquid
M	Model (test facility)
m	Diffusion process temporal scale
net	Net gain or loss
N_2	Nitrogen

Table continued

Subscript or Superscript	Definition
out	Out the control volume in Figure 5.2-1
P	Prototype (plant)
PP	Pump power
ref	Reference
R	Ratio
s	Coolant
s	Surface
S	Specific
sat	Saturation in Figure 5.2-1
sys	System
T	Temperature
t	Time
v	Vapor
$\dot{V}$	Volumetric flow rate effects
wall	Wall
w	Cladding
0	Initial conditions at start of the time sequence, or reference value
$1\phi l$	Single phase liquid in Figure 5.2-1
$1\phi v$	Single phase vapor in Figure 5.2-1
2ϕ	Two phases in Figure 5.2-1
τ	Convection process temporal scale
+	Dimensionless, normalized
.	Rate

1.4.3 Abbreviations

Abbreviation	Definition
CCM	Collection of computer models
COTS	Commercial off-the-shelf program
EM	Evaluation model
EMDAP	Evaluation model development and assessment process
FRC	Fractional rate change
FSA	Fractional scaling analysis
H2TS	Hierarchical, two-tiered scaling system
IETs	Integral effects tests
LBLOCA	Large brake loss of coolant accidents
LOCA	Loss of coolant accidents
NPP	Nuclear power plant
NRC	Nuclear Regulatory Commission
PCT	Peak cladding temperature
PIRT	Phenomena Identification and Ranking Table
PTs	Phenomenological tests
PWR	Pressurized water reactor
SBLOCA	Small break loss of coolant accident
SETs	Separate effects tests
SM	Specific model

2 CREATION OF THE ADEQUACY MATRIX AND VALIDATION MATRIX USING SCALED EXPERIMENTAL FACILITIES

Scaled experimental facilities, both IETs facilities and SETs facilities, are designed, constructed, and operated to generate data for validation. The developed collection of coupled models (CCM) results are compared with obtained IETs and SETs experimental data. However, the CCM results are intended to be used later for performing nuclear power plant calculations to obtain construction and operating licenses. To use CCM for nuclear power plant calculations, an assessment of the CCM adequacy as an additional step is needed. Because NPPs must be shown to be safe during a specific set of scenarios including normal operations and accidents, the data generated using scaled facilities are not only for single steady-state conditions at various power levels, but apply to entire envelopes of operation and accidents. Thus, validation data sets used to calculate the behavior of NPPs are extensive and consist of data sets for each postulated operational and accident scenario. A scenario is defined as the trajectory of the steady-state or transient conditions that are present in the NPP from the starting point of the scenario (often the steady-state operational condition when producing power) to the end point of the scenario (a stable end-state point, such as a cold shutdown). An example of one of the most challenging scenarios is that of the maximum leak scenario which is a complete shear of the largest pipe (approximately 0.86 m diameter) in the system operating at a nominal pressure of 15.7 MPa and 597 K subcooled water temperature after being heated by the core. The system will depressurize to approximately 0.5 MPa in 30 s while experiencing a wide range of thermodynamic conditions, flow regimes, and temperature excursions during the intervening transient. Subsequently, the NPP is taken to a cold shutdown condition that will require hours to achieve.

The data sets obtained from the scaled experimental facilities form validation matrices that provide the basis for validating the software used to perform NPP licensing calculations. Usually, the validation matrix is a subset of the adequacy matrix. The validation matrix is related to the direct comparison of IETs and SETs experimental results and computational model (software) results. The adequacy matrix considers multiple SETs and IETs test results (old and new) combined and obtained at different scales with different distortions. Using scaling analysis and deriving appropriate dimensionless groups, experimental results from several facilities can be combined to provide the data set needed to assess the adequacy of the developed software for the real-world system. See Nonmandatory Appendix A, section A-3 as an example. The process from the point of determining the kinds of data required to be generated in scaled experimental facilities to the point of constructing adequacy matrix and validation matrix for a particular type of scenario for an NPP is shown in simplified form in Figure 2-1.

Once the NPP and the scenario of interest have been selected, Step I in Figure 2-1 is then performed to identify the process used to isolate the key phenomena relevant to quantities of interest[1] using phenomena identification and ranking tables (PIRT). PIRTs are generated to determine the phenomena that must be characterized by the experiment using scaled facilities that have been designed to adequately represent an NPP under investigation for the chosen challenging scenarios.

Step II in Figure 2-1 characterizes the needed data by defining the data range for key phenomena throughout the NPP as a function of the NPP component geometry, thermodynamic states, and boundary conditions. Step III in Figure 2-1 specifies and collects all available data that has been previously obtained from scaled facilities. The data already available are isolated in Step IV in Figure 2-1. By subtracting the data sets already available, as determined in Step III in Figure 2-1 from the data sets needed and defined in Step II in Figure 2-1, the data matrix is defined that determines the extent and specifications of the scaled facilities that must be designed, constructed, and operated. These data are identified in Step V in Figure 2-1.

To satisfy the validation data needed to populate the adequacy and validation matrix, both IET- and SET-scaled facilities are designed (see Step VI in Figure 2-1). Whether the necessary data may be provided via an IET facility (see Step VII in Figure 2-1) or a SET facility (see Step VIII in Figure 2-1) is typically determined based on a strategy centered on the design of a comprehensive IET facility capable of performing both steady-state and transient experiments representing the entire NPP response. The SET facilities are designed (usually closer to the full scale and better instrumented than IET) to complement the data generated in the IET facility with more detailed data tailored to localized regions of interest in key NPP plant components, e.g., the core or steam generator.

Data generated by the scaled IET and SET facilities based on the specifications generated in Step V in Figure 2-1 comprise the missing factors required in the adequacy and validation matrix (see Step IX in Figure 2-1).

[1] The term “figures-of-merit” can be used as a synonym for “quantities of interest” (see ASME VVUQ 1).

Figure 2-1
Process for Creating Assessment Base for Licensing Purposes: Flowchart

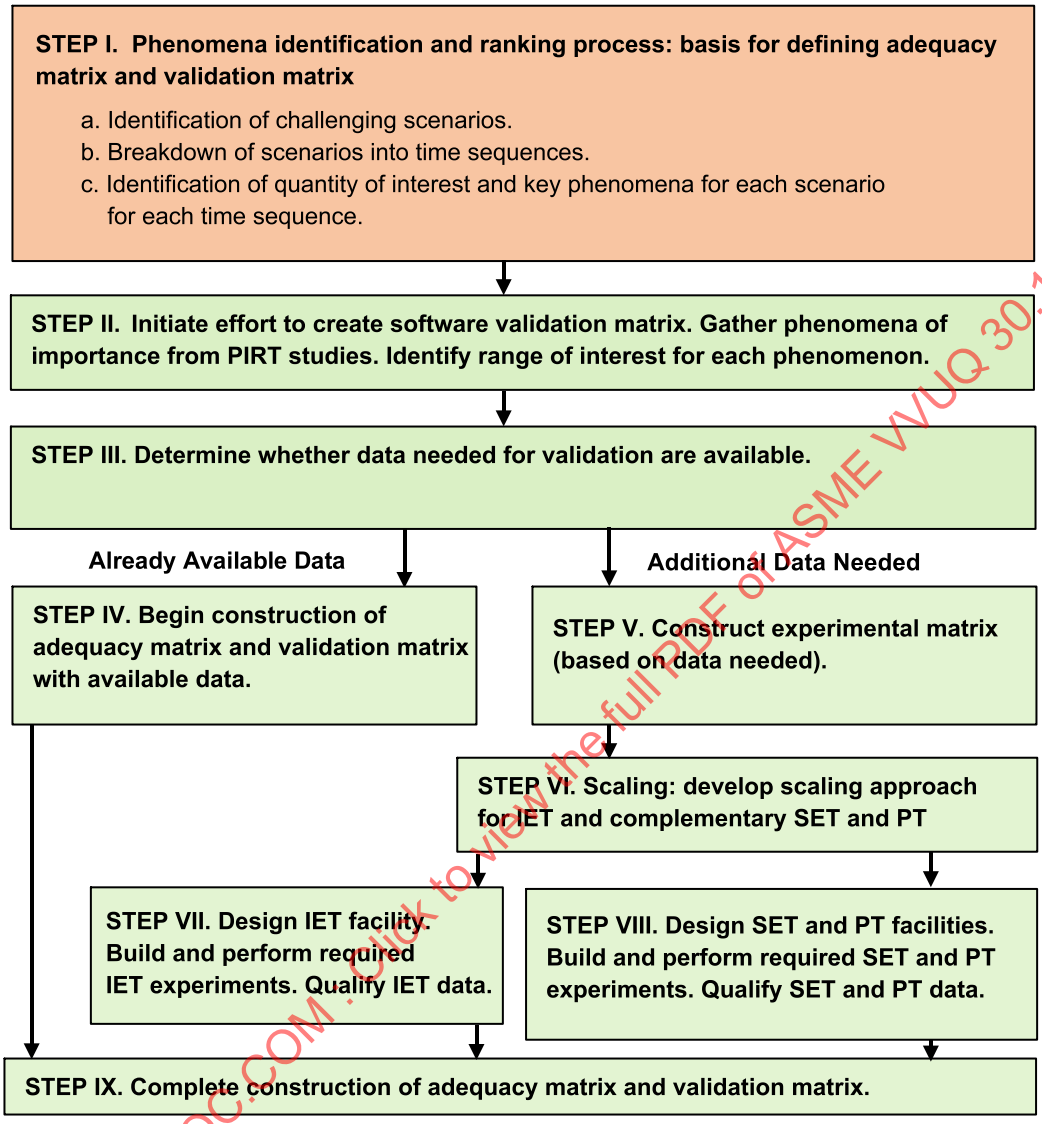

3 SCALING HISTORY AND TYPES

3.1 General

Most systems or control volumes of interest are characterized by quantities of interest and inlet, outlet, and other initial and boundary conditions. For a fluid system, the region of interest is a control volume that is subject to many influences that will affect the characteristics of the control volume. In other fields, the region of interest is a solid body that can deform in the presence of surface forces and internal forces. In the case of the motion of a solid body, friction and external forces govern the quantity of interest such as velocity or acceleration. In all these examples, there is a quantity of interest that characterizes the region under consideration and the set of influences that contribute to the change in the quantity of interest. These influences[2] each have a different impact on the quantity of interest. Some simple examples to illustrate the fractional changes are given by Zuber et al. (2007). A simulation model should predict the contributions of individual influences. Scaling is used to design experiments that identify the ranking of influences in terms of their contributions. Scaling also preserves this ranking between the actual application and surrogate tests. This ensures the relevance of data for the validation of developed models.

[2] These influences are sometimes called forcing functions.

Scaling methodology as applied to complex systems continues to evolve. This section presents a review of past and current practices and recent contributions to scaling for nuclear power system evaluation models and validation experiments.

Aimé Vaschy and Edgar Buckingham developed Pi theorem in 1892 and 1914, respectively, based on the original work of mathematician Joseph Bertrand in 1878. Pi theorem states that if there are n variables in a problem and these variables contain m primary dimensions (for example, for mass, M; length, L; temperature, T; and time, t) the equation relating all of the variables will have $(n - m)$ dimensionless groups. This theorem provides the nondimensional groups that should be matched for scaling, synthesizing data, or developing an empirical correlation from the data.

The advantage of Pi theorem is that equations representing processes are not necessary and only variables of the problem need to be specified to obtain the nondimensional groups. However, this can also be a disadvantage because some important processes and representing variables might not be considered and specified. Consequently, application of Pi theorem is limited to PTs and SETs with a small number of processes and representing variables. However, NPPs consist of multiple interacting control volumes with multiple processes. Thus, for complex systems, such as NPPs, different scaling analysis approaches based on the nondimensional equations for various control volumes and processes are needed (Dzodzo et al., 2019; Wulff and Rohatgi, 1998). Also, even for simpler configurations such as PTs and SETs, the approaches based on the nondimensional equations and selection of only important phenomena can provide a reduction of the necessary dimensionless groups (see, for example, Catton et al., 1990 and 2009, and Nonmandatory Appendix A, section A-5).

The majority of IET facilities in the past were scaled based on the volumetric scaling approach and keeping the ratio of power to volume in the model the same as in the prototype. An overview of test facilities built based on volumetric scaling approach is presented in (Glaeser and Karwat, 1993). This document gives a brief overview (see section 3.2) of the basics as well as advantages and disadvantages of the volumetric scaling approach.

Subsequently, the scaling was structured into a hierarchy due to the increased complexity of systems, subsystems, modules, and multiple phenomena. The hierarchy allows the system under consideration (i.e., the control volume) to be shifted as necessary. Zuber (1991) and Ishii and Kataoka (1984) have both proposed forms of scaling for nuclear power systems organized by hierarchy, and Zuber's hierarchical, two-tiered scaling (H2TS) system is an example of this basic approach to scaling organization that has been used to assess evaluation models used for reactor license simulations. An additional scaling method called fractional scaling analysis (FSA) was proposed by Wulff et al. (2009) and Zuber et al. (2007). The FSA addresses acknowledged weaknesses in earlier embodiments of scaling for nuclear power systems. H2TS and FSA are discussed in section 4.

The approach described in the evaluation model development and assessment process (EMDAP) in Regulatory Guide 1.203 (2005) invokes scaling arguments for data selection and experiment design. However, the evaluation model is not used to inform the scaling efforts. D'Auria and Galassi (2010) offer another structure for implementing scaling of the experiments for the assessment of nuclear power system models that use CCM for the scaling and design of test facilities.

One example is a three-level scaling approach by Ishii et al. (1998) and triad method scaling approach by Ransom, Wang, and Ishii (1998) where three separate computer models for the prototype, an ideal scaled model and scaled test facilities were used. Another example where the evaluation model was used to support scaling efforts and design of the test facility is presented in Achili et al. (2011).

An overview of scaling analyses approaches and the new trends and developments in scaling analysis is presented in the Organisation for Economic Co-operation and Development's report NEA/CSNI/R(2016)14 (2017). The main difference between NEA/CSNI/R(2016)14 and this Standard is that this Standard is focused only on the scaling analysis needed to develop and design IET and SET facilities and evaluate effects of their distortions. Also, Nonmandatory Appendix A provides examples of scaling analysis applications.

3.2 Volumetric Scaling Approach

The majority of IET facilities in the past were scaled based on keeping the ratio of power-to-volume in the model the same as in the prototype. If the integral test facility operates at prototypical pressure with the same fluid and residence time, the power-to-volume scaling criterion is as follows:

$$[q'' \times A_T/V_{\mathrm{CV}}]_M = [q'' \times A_T/V_{\mathrm{CV}}]_P \tag{3-1-1}$$

where

A_T = transport area
q'' = heat flux
V_{CV} = control volume

Subscripts M and P indicate model (scaled test facility) and prototype (full-scale nuclear power plant), respectively.

The volumetric scaling approach can be a first step (attempt) in scaling and supporting preliminary design of the test facilities. H2TS, or FSA, or some other scaling methodologies can be used subsequently to refine design of the test facility and quantify and decrease scaling distortions.

The volumetric scaling approach has some advantages, but also some disadvantages. Besides scaling the volume, prototypical height test facilities are usually used. Figure 3.2-1 shows the schematics of the LOFT and Semiscale facilities that use the volumetric scaling approach for the pressurized water reactor (PWR) at different volumetric and height scales. Comparison of the two facilities shows that for smaller $V_R = V_M/V_P$ and $H_R = 1$ all vessels have the shape of elongated vertical cylinders.

3.2.1 Advantages of the Volumetric Scaling Approach

3.2.1.1 Prototypical Height. The use of prototypical height enables

(a) prototypical distance between the heat source and heat sink centers to properly simulate natural convection effects

(b) both single-phase and two-phase natural convection loops to be simulated simultaneously

(c) prototype and model fluid average cross-section velocities and residence times in the loops to be the same

(d) horizontal interphase areas (transfer area concentrations) to be properly scaled

3.2.1.2 Prototypical Pressure and Temperature. When using prototypical pressure and temperature, distortions due to the different fluid properties are not present (scaling analysis does not generate additional terms related to property distortions). This allows for easier interpretation of the results.

3.2.2 Disadvantages of the Volumetric Scaling Approach. The disadvantages of the volumetric scaling approach are as follows:

(a) If volume ratio of model (test facility) and prototype (plant) $V_R = V_M/V_P$ is small, the ratio of the test facility and plant vertical side wall areas decreases only $(V_M/V_P)^{1/2}$ times. Test facility volumes become elongated narrow cylinders if factor $V_R = V_M/V_P$ is small and the height of the facility (model), H_M, is the same as the height of the prototype, H_P, i.e., $H_R = 1 (H_M = H_P)$ [for comparison, see Figure 3.2-1, illustrations (a) and (b)]. Consequently, the transfer area for heat transfer and friction on the test facility vertical side walls is larger than needed.

(b) In the case of low volume ratios, V_R, [see Figure 3.2-1, illustration (b)] and the same heights, $H_M = H_P$, some flow regimes and three-dimensional effects cannot be simulated due to the elongated or narrow domains (flow paths).

(c) Some components (e.g., heat exchangers) might be represented with a limited number of tubes, which is not adequate to address bundle effects.

SETs might be needed to overcome these disadvantages. For example, some components of the IET, like the reactor vessel, steam generator, containment, or heat exchangers, may be separately tested. Also, portions of components including fuel assemblies and steam generator bundles might be tested to check and derive heat and mass transfer correlations, establish critical heat flux, test fluid-structure interaction effects, etc.

4 OVERVIEW AND COMPARISON OF H2TS AND FSA SYSTEM DECOMPOSITION AND HIERARCHY

H2TS and FSA methodologies use concepts from the hierarchical theory initially presented by Mesarovic, Macko, and Takahara (1970). Both methodologies decompose the system into multiple control volumes.

The H2TS analysis methodology (Zuber, 1991; Zuber et al., 1998) decomposes the system and establishes a hierarchy as presented in Figure 4-1.

FSA (Zuber et al., 2007) formally decomposes the system to only the following three levels:

(a) system (S)

(b) components (SS and M)

(c) process (P_i)

However, to perform detailed FSA and locate the most important processes, information about constituents (C), phases (P), geometrical configurations (GC), and fields (F) can be needed as well.

Four stages of H2TS are presented in Figure 4-2. Stage 3 top-down system scaling analysis and Stage 4 bottom-up process scaling analysis might be repeated iteratively several times. A similar flowchart can be applied for FSA.

Figure 3.2-1
Comparison of Elongated Representations of Volumes in LOFT and Semiscale Mod-2A Test Facilities

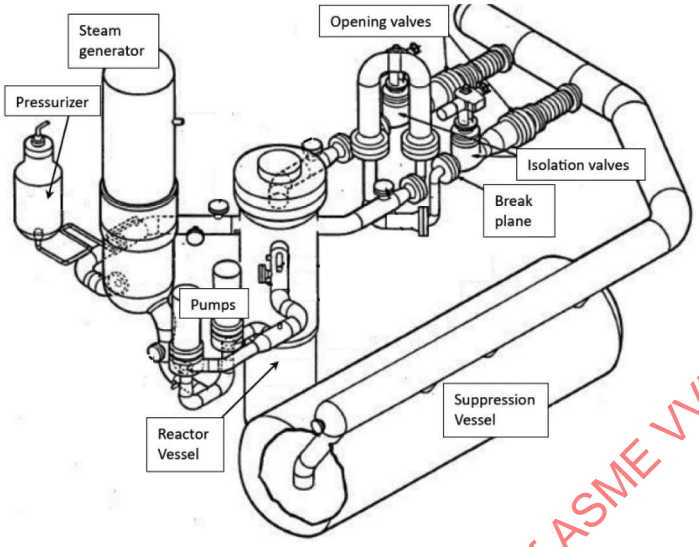

(a) LOFT (Reeder, 1980) [Note (1)]

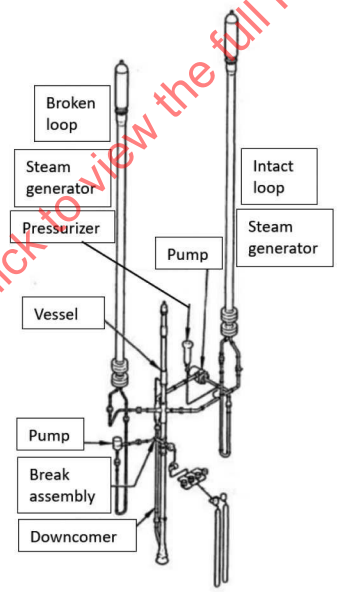

(b) Semiscale Mod-2A (Loomis, 1987) [Note (2)]

NOTES:
(1) LOFT test facility volume scale: $V_R = V_M/V_P = 1/60$; height scale $H_R = H_P/H_M = 0.5$
(2) Semiscale Mod-2A volume scale: $V_R = V_M/V_P = 1/1705$; height scale $H_R = H_P/H_M = 1$

Figure 4-1
System Decomposition and Hierarchy for Processes Applied in H2TS

System decomposition	Hierarchy for processes									Hierarchy for length, time, and volumetric concentration
System (S)	S									$(SS_1,..., SS_k)$ L_S, τ_S, α_S
Subsystem (SS)	SS_1								SS_k	$(M_1,..., M_k)$ L_{SS}, τ_{SS}, α_{SS}
Modules (M)	M_1							M_k		$(C_1,..., C_k)$ L_M, τ_M, α_M
Constituents (C)	C_1						C_k			(g, f, s) L_C, τ_C, α_C
Phases (P)	g					f	s			$(G_1,..., G_k)$ L_{CP}, τ_{CP}, α_{CP}
Geometrical configurations (G)	G_1				G_k					(M, MM, E) L_{CPG}, τ_{CPG}, α_{CPG}
Fields (F)	M	MM	E							$(P_1,..., P_k)$
Processes			P_1	P_k						L, τ

GENERAL NOTE: Modified from Zuber, 1991.

Figure 4-2
Four Stages of H2TS

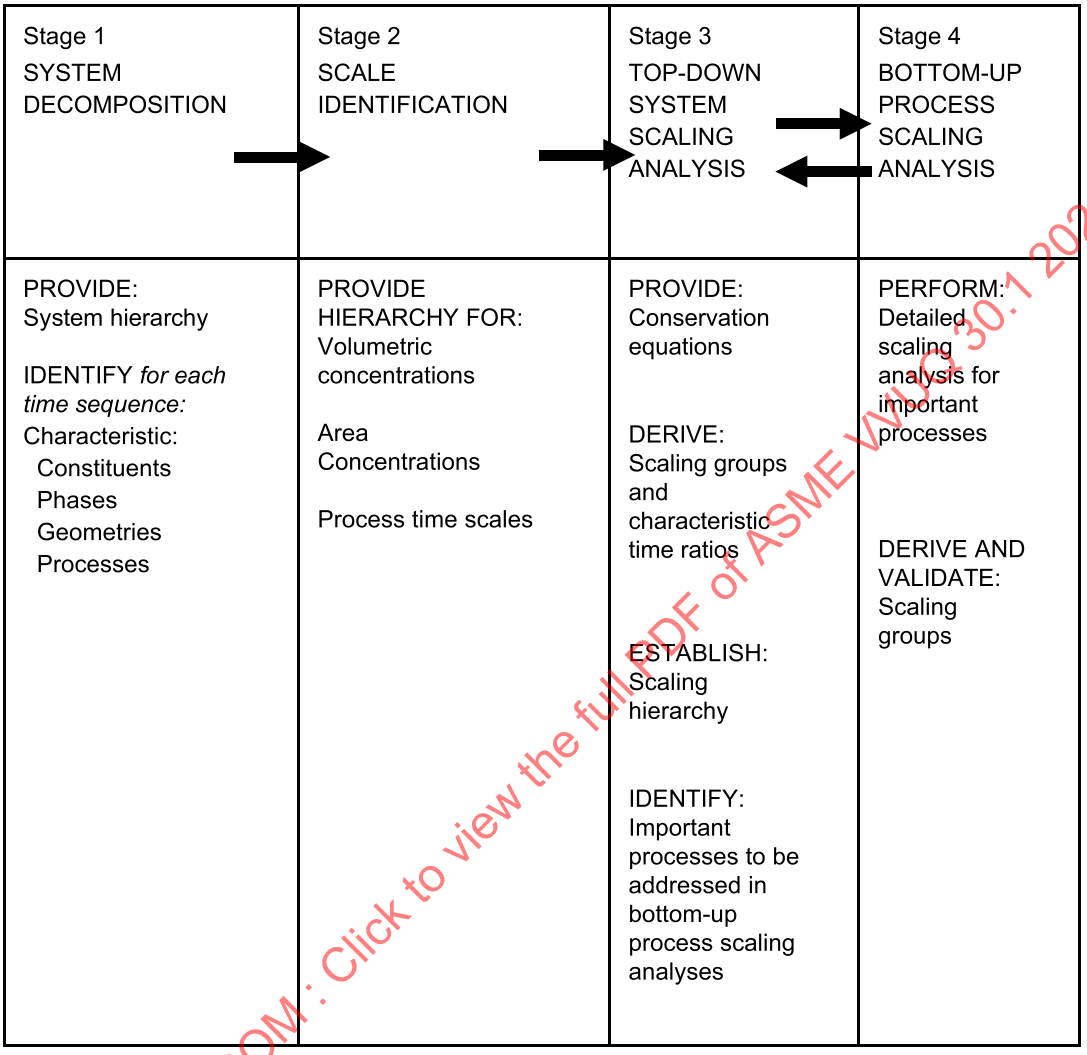

GENERAL NOTE: Modified from Zuber, 1991.

5 CONCEPT OF TIME–SCALE MODELING — DIMENSIONLESS GROUPS IN TERMS OF TIME RATIOS

5.1 Introduction

The concept of time–scale modeling is used to analyze large and complex power systems. The concept is presented in Chow (1986) and Kline (1986). The scaling groups can be represented as the products of frequencies and times, or ratios of two frequencies:

$$\Pi_{\mathrm{Re}} = \omega \times \tau = \frac{\omega_1}{\omega_2} \tag{5-1-1}$$

The advantage of time scaling is that multiple scaling groups needed for complex systems are derived using the same approach and can be directly compared. For example, for convective process the time can be the fluid residence time in the control volume. Also, the reciprocal value of the residence time is the frequency of fluid replacement in the control volume.

However, traditional scaling groups, derived from dimensionless equations, associated with steady state phenomena may also be usefully decomposed into ratios of time scales.

For example, for the control volume consisting of the pipe segment length, L, equal to the pipe diameter, D, ($L = D$), the connection between the "new" time-based dimensionless group formulation and the Reynolds number, Re, as a ratio of inertial forces to viscous forces influences (as presented in dimensionless Navier-Stokes equations), is illustrated using the following equation (Dzodzo, 2019):

$$\Pi_{\mathrm{Re}} = \mathrm{Re} = \frac{\rho v \dfrac{\partial v}{\partial x}}{\mu \dfrac{\partial^2 v}{\partial x^2}} \sim \frac{\bar{v}\dfrac{\bar{v}}{L}}{\nu \dfrac{\bar{v}}{L^2}} = \frac{\bar{v} \times L}{\nu} = \frac{\bar{v}^2}{\nu} \times \frac{L}{\bar{v}} = \omega \times \tau \tag{5-1-2}$$

The frequency ω is equivalent to $\bar{v}^2/\nu$ and the residence time τ can be represented by

$$\tau = \frac{L}{\bar{v}} = \frac{A \times L}{A \times \bar{v}} = \frac{V_{\mathrm{CV}}}{\dot{V}} \tag{5-1-3}$$

Thus, the time–ratio relation to the Reynolds number, Π_{Re}, combines the processes ω (inertia and viscous forces effects) and system τ (fluid particle residence time inside the system) points of view. Thus, the Reynolds number presented as a product of frequency and time can be used in the time–scaling concept and compared with all other dimensionless groups based on the products of time ratios. This approach can produce numerous comparable dimensionless groups and enable analysis of large and complex systems.

Examples of H2TS and FSA dimensionless groups derivations are available in section 5.3 and Nonmandatory Appendix A, sections A-1 and A-2.

The derivation of dimensionless groups is based on nondimensional equations for multiple control volumes and processes present in NPPs during various time sequences of the postulated accident scenarios. This part of scaling analysis is based on PIRT, and it is important that all processes and relevant phenomena are included in the equations. Each derived dimensionless group is an analytical solution and the results depend on the skills of the analyst to derive, adjust, and derive nondimensional equations. It is important that all equations and derived dimensionless groups are obtained using the same procedure so that dimensionless groups are comparable and not dependent on the arbitrary choice of relevant variables (as for example in Pi theorem applications). Based on the established quantities of interest the relevant equations for scaling analysis can be derived by combining mass, momentum, and energy balance equations. For example, the reactor vessel pressure response and the reactor vessel water level equations (see Nonmandatory Appendix A, sections A-3 and A-4) can be derived by combining mass and energy balance equations.

The last step in scaling analysis is quantification of the dimensionless groups. The comparison of the quantified dimensionless groups provides an evaluation of the significance of processes and phenomena. Also, the comparison of the quantified dimensionless groups for the same processes and phenomena present in prototype and models provides the quantitative evaluation of the model experimental results applicability and distortion. At this point the scaling analysis depends on the previously performed uncertainty evaluation of experimental results considering uncertainties of measurement, applied materials thermophysical properties correlations, instrumentation calibrations, and other testing uncertainties (ASME PTC 19.1-1998; Guide to the Expression of Uncertainty in Measurement, 1995). Also, in the case of the quantification of prototype dimensionless groups, it is often necessary to use either interpolation

or extrapolation of the test results obtained with several test facilities built with different scale factors and operated at different fluid conditions. These uncertainties need to be evaluated previously as well.

Experimental results for various accident scenarios based on the prototype scale and conditions exist but are limited. They are usually obtained by using old and decommissioned plants as test facilities. Some examples for the reactor vessels are presented in Glaeser and Karwat (1993) and Wulff and Rohatgi (1998); some examples for containment vessels are presented in Cron and Schrammel (1993) and Woodcock and Dzodzo (2000). However, usually the dimensions and conditions of the new designs are not the same and experimental results need to be either interpolated or extrapolated. A CCM which is already verified, validated, and assessed adequately can be used to perform calculations for the prototypical configuration and conditions and quantify dimensionless groups. Also, the same CCM can be used to support the design of the scaled test facilities (Achili et al., 2011; Ishii et al., 1998; Ransom, Wang, and Ishii, 1998). However, in that case the eventual limitations (such as heat transfer correlations and applied correlations for material properties) and uncertainties of the CCM results related to the quantified dimensionless groups need to be evaluated.

5.2 Scale Identification

Stage 2 (scale identification) for H2TS is presented in Figure 4-2. The volumetric concentrations, transfer area concentrations, and process time scales need to be obtained for each hierarchical level.

For FSA, the scale identification stage is different due to the smaller number of hierarchical levels and the different integral approach needed to derive equations based on the summation of agents of change effects. Instead of establishing volumetric and area concentrations and time scales for each hierarchical level, it is important to have information of the ratios of subvolumes occupied by single-phase liquid $V_{1\phi l}$, single-phase vapor $V_{1\phi v}$, saturated two-phase mixture $V_{2\phi}$ and noncondensable nitrogen gas V_{N2}, inside the system volume (where $V = V_{1\phi l} + V_{1\phi v} + V_{2\phi} + V_{N2}$) as shown in Figure 5.2-1, so that compressibility of each subvolume can be taken into account (Wulff and Rohatgi, 1998).

In reference to Figure 5.2-1, the following must be considered in the system control volume V:

(a) Each subvolume, $V_{1\phi l}$, $V_{1\phi v}$, $V_{2\phi}$, V_{N2}, may change in time, but the total volume V is constant.

(b) Subvolumes may interchange mass (e.g., mass flow rate terms $\dot{m}_{1\phi v,\mathrm{sat}\rightarrow 1\phi v}$ or $\dot{m}_{1\phi l\rightarrow 1\phi l,\mathrm{sat}}$) and energy [see heat transfer terms $(\dot{Q}_{N_2,1\phi v})_{\mathrm{int}}$, $\left(\dot{Q}_{1\phi v,2\phi}\right)_{\mathrm{int}}$, $(\dot{Q}_{N_2,2\phi})_{\mathrm{int}}$, $(\dot{Q}_{N_2,1\phi v})_{\mathrm{int}}$, $\left(\dot{Q}_{1\phi v,2\phi}\right)_{\mathrm{int}}$] at the subvolumes boundaries.

(c) Each subvolume can exchange heat with the surrounding walls (i.e., $\dot{Q}_{1\phi v,\mathrm{wall}}$, $\dot{Q}_{N_2,\mathrm{wall}}$, $\dot{Q}_{2\phi,\mathrm{wall}}$, $\dot{Q}_{1\phi l,\mathrm{wall}}$).

(d) The subvolumes may be placed anywhere in the control volume and need not necessarily be continuous (e.g., summation of all bubble volumes can represent one subvolume).

(e) There can be mass flow rates terms ($\dot{m}_{1\phi v,\mathrm{in}}$, $\dot{m}_{1\phi v,\mathrm{out}}$, $\dot{m}_{N_2,\mathrm{in}}$, $\dot{m}_{N_2,\mathrm{out}}$, $\dot{m}_{2\phi,\mathrm{in}}$, $\dot{m}_{2\phi,\mathrm{out}}$, $\dot{m}_{1\phi l,\mathrm{in}}$, $\dot{m}_{1\phi l,\mathrm{out}}$) related to each field entering or exiting the control volume.

(f) Subcooled liquid, two-phase mixture, vapor, or noncondensable gas can be discharged from, or into, the control volume (see term $\sum_{j=bk}\dot{V}_j$ for various break-flow volumetric flow rates).

All specified information needs to be extracted from the applied evaluation models (used to support scaling analysis) and later from the test facility so that comparisons between analysis and test results will be possible. Based on this, special attention needs to be taken in planning an adequate two-phase flow measurement in piping between test facility components (tanks), as well as collapsed water level and void distributions inside the components.

The control volume in Figure 5.2-1 is applied in Nonmandatory Appendix A, section A-3 for reactor vessel pressure response and Nonmandatory Appendix A, section A-4 for the reactor water level response.

5.3 Top-Down Approach — Scaling Hierarchy

5.3.1 H2TS. In H2TS, the control volume balance equation for constituent i is

$$\frac{dV_i\psi_i}{dt} = \Delta[\dot{V}_i\psi_i] \pm \sum_{k=1}^{m-1}\left(j_{ik}A_{ik}\right) + S_i \qquad (5\text{-}3\text{-}1)$$

where ψ_i is the state variable (quantity of interest) of constituent i in volume V_i

for mass: $\psi = \rho$

for momentum: $\psi = \rho\vec{v}$

for energy: $\psi = \rho \times e$

Figure 5.2-1
Subvolumes, V_i, and Control Volume, V

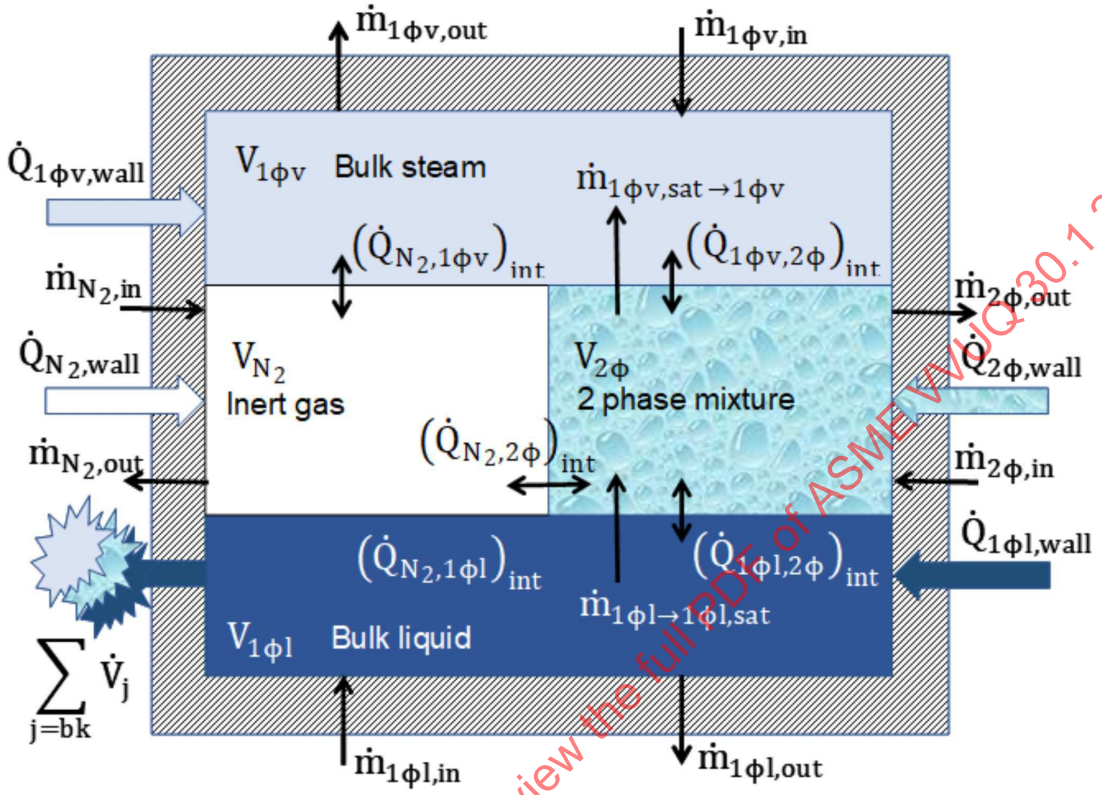

GENERAL NOTE: The figure is provided courtesy of the *Journal of Nuclear Engineering and Radiation Science* (Dzodzo et al., 2019) and based on Wulff and Rohatgi (1998).

After substituting variables in dimensionless form (e.g., $V_i^+ = V_i/V_{i,0}$, $\psi_i^+ = \psi_i/\psi_{i,0}$) and normalizing the equation with the convective term $\dot{V}_{i,0}\psi_{i,0}$, the dimensionless form is

$$\tau_i \frac{dV_i^+\psi_i^+}{dt} = \Delta[\dot{V}_i^+\psi_i^+] \pm \sum_{k=1}^{m-1}\left(\Pi_{ik} j_{ik}^+ A_{ik}^+\right) + \Pi_{sk} S_i^+ \quad (5\text{-}3\text{-}2)$$

where

τ_i = residence time of constituent i in volume V_i

$$\tau_i = \frac{V_{i,0}}{\dot{V}_{i,0}} \quad (5\text{-}3\text{-}3)$$

Each specific time ratio for a transfer process between constituents i and k is composed of a specific frequency and residence time of constituent i in volume V_i:

$$\Pi_{ik} = \frac{j_{ik,0}A_{ik,0}}{\dot{V}_{i,0}\psi_{i,0}} = \left(\frac{j_{ik,0}A_{ik,0}}{V_{i,0}\psi_{i,0}}\right)\left(\frac{V_{i,0}}{\dot{V}_{i,0}}\right) = \omega_{ik}^S \tau_i \quad (5\text{-}3\text{-}4)$$

The comparison of the time ratios values provides an evaluation of a significance of processes on the response of constituent *i*. The time–ratio magnitude scales with the importance of transfer process. Thus, after quantifying all time ratios, all processes might be ranked based on their importance on the system. This quantification and comparison might support or revise PIRT and decrease the number of processes which need to be simulated in the test facility (if they are not important to the system response). Thus, the top-down system approach provides a method for establishing a scaling hierarchy.

The most important time ratios must be preserved for the prototype and the model ($\Pi_M = \Pi_P$). The distortion in the model can be estimated as in Zuber (1991):

$$D = \frac{\Pi_P - \Pi_M}{\Pi_P} \tag{5-3-5}$$

When this formulation is applied, the distortion needs to be as close as possible to zero.

Another way to estimate distortions is to calculate ratios of dimensionless groups as in Wulff et al. (2009):

$$D = \frac{\Pi_M}{\Pi_P} \tag{5-3-6}$$

In this case, the distortion needs to be as close as possible to one.

In the case that the distortion is $|D| > 1$ [based on eq. (5-3-5)] or $D < 0$ [based on eq. (5-3-6)] the signs for Π_P and Π_M are different. This indicates that phenomena in the prototype and model are opposite. For example, heat loss instead of heat gain, or condensation instead of evaporation are present in the model. These situations should be avoided, or the appearance and duration should be minimized so that transfer processes play essentially the same role in the model as in the prototype.

Some examples of H2TS applications related to two-phase flows in complex systems are available in Levy (1999).

5.3.2 FSA. The FSA equation for the time derivative of a state variable (quantity of interest) Ψ_i is derived as a summation over all agents of change (in fact influences) ϕ_j:

$$\frac{d\Psi_i}{dt} = \sum_{j=1,n} \left(\frac{d\Psi_i}{dt}\right)_j = \sum_{j=1,n} \Phi_j \tag{5-3-7}$$

For example, if the state variable is energy $\Psi_i = E$, the change of energy per time will be equal to the summation of all agents of change (influences) that are, in this case, the power of sources or sinks $\phi_j = P_j$.

The fractional rate of change (FRC) ω_j of state variable Ψ_i caused by agent of change ϕ_j is represented by

$$\omega_j = \frac{\left(\frac{d\Psi_i}{dt}\right)_j}{\Psi_i} = \frac{\Phi_j}{\Psi_i} \tag{5-3-8}$$

Then eq. (5-3-7) in dimensionless form is

$$\frac{d\Psi_i^+}{dt^+} = \sum_{j=1,n} \frac{\omega_j}{|\bar{\omega}|} \times \Phi_j^+ \tag{5-3-9}$$

where

t^+ = dimensionless time
= $|\bar{\omega}| \times t$

$|\bar{\omega}|$ = effective FRC of the system
= $\left|\sum_{j=1,n} \omega_j\right|$

To quantify the effect of a change in state variable (quantity of interest) Ψ_i in control volume by an amount $\delta\Psi_i$, the reference value Ψ_0 can be used to define fractional change (effect metric), Ω_j, as

$$\Omega_j = \frac{\delta\Psi_i}{\Psi_0} = \frac{\omega_j \times \Psi_i \times \delta t}{\Psi_0} = \frac{\Phi_j}{\Psi_0}\,\delta t \tag{5-3-10}$$

Examples for various state variables, agents of changes, FRCs, and fractional changes (effect metrices) are available in Nonmandatory Appendix A, section A-2.

Practitioners are cautioned that the state variables are coupled, so FRC evaluations should consider all state variables, not just measurable or measured state variables. The advantage of this derivation, compared to the classical control volume approach in H2TS (where dimensionless numbers Π are derived by nondimensionalization of equations for state variables), is that each process is represented with its own agent of change.

Thus, the ratios of fractional rates of change, normalized fractional changes (effect metrics), $\Omega_j^+ = \omega_j/|\bar{\omega}|$, might be easier used for PIRT quantification.

The distortion of each process (agent of change) might be evaluated as in Wulff and Rohatgi (1998):

$$D_j = \frac{\Omega_{j,M}^+}{\Omega_{j,P}^+} \quad j = 1, n \tag{5-3-11}$$

The distortion acceptability criteria might depend on the specified quantities of interest and design of IET facilities or SETs. Also, even for the same IET facility and the same transient simulation, the criteria might be different for various time sequences depending on the number of important (dominant) agents of change (influences) ϕ (effect metrics Ω). If only one dominant agent of change exists during a one-time sequence, the distortion acceptability criteria need to be preserved for the corresponding effect metric ratio. The most complex case for the time sequences occurs when all agents of change are of almost equal importance and the distortion acceptability criteria need to be preserved for all corresponding effect metric ratios.

The synthesis of parameters governing the process is achieved by deriving and quantifying the effect metric Ω. At the component level, the synthesis is performed on processes and the effect of each process on a state variable is analyzed by comparing the magnitude of corresponding effect metric Ω to the effect metric of the other processes. The important processes that must be modeled in codes and present in test facilities are identified for each component in each row of the system matrix presented in Figure 5.3.2-1.

At the system level, the synthesis is performed on system components via a system matrix as shown in Figure 5.3.2-1 where rows are for the components and columns are for their processes. The system matrix is different for different time sequences and the hierarchy of processes needs to be generated for each time sequence.

A recommendation of distortion acceptability criteria for one specific example is presented in Wulff and Rohatgi (1998). One example of FSA application for derivation of time rate depressurization equation is presented in Wulff et al. (2009).

5.4 Combination of H2TS and FSA Approaches

The comparison of dimensionless groups derived in H2TS and FSA, as shown in eqs. (5-3-4), (5-3-7), and (5-3-8) leads to the conclusion that these two approaches can be combined.

It can be concluded that specific frequency ω_{ik}^S in eq. (5-3-4) is an analog of FRC ω in eq. (5-3-8):

$$\left(\frac{j_{ik,0}A_{ik,0}}{V_{i,0}\psi_{i,0}}\right) = \omega_{ik}^S = \frac{\left(\frac{d\Psi}{dt}\right)}{\Psi} = \frac{\Phi}{\Psi} = \omega \tag{5-4-1}$$

In eq. (5-4-1), the nominator, $j_{ik,0}A_{ik,0}$, corresponds to an agent of change $j_{ik,0}A_{ik,0}$, = $d\Psi/dt$ = ϕ and the denominator, $V_{i,0}\psi_{i,0}$, corresponds to the state variable Ψ.

The period δt in eq. (5-3-10) can be the residence time $\tau_i = V_{i,0}/\dot{V}_{i,0}$ as in eqs. (5-3-2) to (5-3-4), or some other reference period $\delta t = \Delta t_{ref}$.

Thus, in some cases, the derived dimensionless groups in H2TS and FSA are the same:

$$\Pi_i = \Omega_i \tag{5-4-2}$$

This approach can be used to quantify dimensionless groups in H2TS and relate them to only one process (instead of the combination of several processes). Also, the equations based on the FSA approach can be derived for the hierarchical level of interest, e.g., the system level. Wulff and Rohatgi (1998) contains some examples.

On the other hand, the FSA approach can be used to derive equations at various hierarchical levels (as in H2TS) if the intent is to scale SETs when several processes, fields, geometrical configurations, phases, and constituencies are present.

Examples of the reactor vessel pressure and water level responses are presented in Nonmandatory Appendix A, sections A-3 and A-4.

Figure 5.3.2-1
Changes of System Matrix for FSA During the Duration of NPP Transient

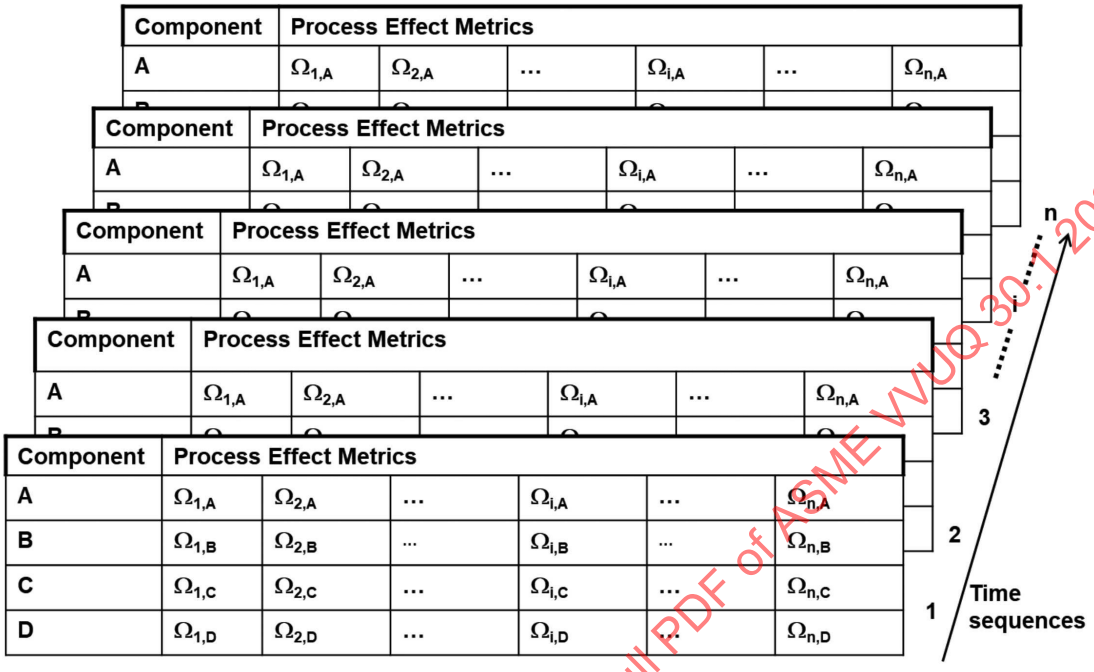

GENERAL NOTE: The figure is provided courtesy of the *Journal of Nuclear Engineering and Radiation Science* (Dzodzo et al., 2019) and based on Wulff and Rohatgi (1998).

5.5 Bottom-Up Approach

The bottom-up approach is performed only for the processes that are identified as being important to the behavior of the system in the case of IET, or component (or module) in the case of SET. Thus, the bottom-up analysis is focused on the specific processes and quantification of flux and geometrical terms present in nondimensional groups.

According to Zuber (1991, p. D-62) the bottom-up approach has the following three important objectives:

(a) to discern the mechanisms that govern the flux and geometrical terms

(b) to establish and validate functional relations for calculating these terms

(c) to demonstrate that these fractional relations (or models) can be applied to a full-scale system

Important objectives and steps of the bottom-up approach are listed in Zuber (1991, pp. 19–20). For example, the applicability of correlations for heat and mass transfer present in the evaluation model needs to be confirmed for both, plant, and model conditions. The detailed analysis of governing mechanisms ensures that processes important to system response are adequately addressed. The bottom-up scaling also confirms assumptions regarding processes that are neglected (to establish sufficiency of scaling).

5.6 Two-Tiered Approach

The top-down approach scales the behavior of the whole system and establishes important processes. In the bottom-up approach, the effects of the important specific processes are investigated and quantified at the lower levels. Thus, the top-down approach provides efficiency and the bottom-up provides the sufficiency of the scaling analysis.

Examples of the two-tiered approach are available in Ishii et al. (1998) and Reyes and Hochreiter (1998). In Ishii et al., the dimensional groups were derived by using linear small-perturbation analysis, while in Reyes and Hochreiter, H2TS analysis was applied.

MANDATORY APPENDIX I
REFERENCES

The following is a list of publications considered and referenced in this Standard:

Achili, A., Congiu, C., Ferri, R., Bianchi, F., Meloni, P., Grgic, D., and Dzodzo, M. (2011). "SPES3 Facility RELAP5 Sensitivity Analyses on the Containment System for Design Review." Science and Technology of Nuclear Installations, 2012, Article 173637. https://doi.org/10.1155/2012/173637

ASME PTC 19.1-1998. Test Uncertainty. The American Society of Mechanical Engineers.

ASME VVUQ 1. Verification, Validation, and Uncertainty Quantification Terminology in Computational Modeling and Simulation. The American Society of Mechanical Engineers.

Bertrand, J. (1878). *"Sur l'homogénéité dans les formules de physique." Comptes Rendus*, 86(15), 916–920.

Buckingham, E. (1914). "On Physically Similar Systems; Illustrations of the Use of Dimensional Equations." Physical Review, 4, 345–376.

Catton, I., Duffey, R. B., Shaw, R. A., Boyack, B. E., Griffith, P., Katsma, K. R., Lellouche, G. S., Levy, S., Rohatgi, U. S., Wilson, G. E., et al. (1990, May). "A Physically Based Method of Estimating PWR Large Break Loss of Coolant Accident PCT." Nuclear Engineering and Design, 119(1), 109–117.

Catton, I., Wulff, W., Zuber, N., and Rohatgi, U. (2009, December). "Application of Fractional Scaling Analysis to Loss of Coolant Accidents: Component Level Scaling for Peak Clad Temperature." Journal of Fluids Engineering, 131(12), Article 121401. https://doi.org/10.1115/1.4000370

Chow, T. H. (Ed.) (1986). Time Scale Modeling of Dynamic Networks and Applications to Power Systems. Springer Verlag.

Cron, T., and Schrammel, D. (1993, March). Investigations on Hydrogen Distribution in a Reactor Containment, Quick Look Report, Test Group E11, Experiments E11.0-6 (PHDR Technical Report 111–92; in German). Karlesruhe, FRG.

D'Auria, F., and Galassi, G. M. (2010). "Scaling in Nuclear Reactor System Thermal Hydraulics." Nuclear Engineering and Design, 240(10), 3267–3293.

Dzodzo, M. (2019). "Scaling Analysis and Relation to EMDAP and BEPU." Nuclear Engineering and Design, 353, Article 110228. https://doi.org/10.1016/j.nucengdes.2019.110228

Dzodzo, M. B., Oriolo, F., Ambrosini, W., Ricotti, M., Grgic, D., Ferri, R., Achilli, A., Bianchi, F., and Meloni, P. (2019, October). "Application of Fractional Scaling Analysis for Development and Design of Integral Effects Test Facility."ASME Journal of Nuclear Engineering and Radiation Science, 5(4), Article 041208. https://doi.org/10.1115/1.4042496

Glaeser, H., and Karwat H. (1993). The Contribution of UPTF Experiments to Resolve Some Scale-Up Uncertainties in Countercurrent Two Phase Flow. Nuclear Engineering and Design, 145, 63–84.

Guide to the Expression of Uncertainty in Measurement (1st ed.) (1995). International Organization for Standardization.

Ishii, M., and Kataoka, I. (1984). "Scaling Laws for Thermal-Hydraulic System Under Single Phase and Two-Phase Natural Circulation." Nuclear Engineering and Design, 81, 411–425.

Ishii, M., Revankar, S. T., Leonardi, T., Dowlati, R., Bertodano, M. L., Babelli, I., Wang, W., Pokharna, H., Ransom, V. H., Viskanta, R., et al. (1998). "The Three-Level Scaling Approach With Applications to the Purdue University Multi-Dimensional Integral Test Assembly (PUMA)." Nuclear Engineering and Design, 186, 177–211.

Kline, S. T. (1986). Similitude and Approximation Theory. Springer.

Levy, S. (1999). "Testing Two-Phase Flow in Complex Systems." Two-Phase Flow in Complex Systems (Chapter 2). John Wiley & Sons.

Loomis G. G. (1987, July). Summary of the Semiscale Program (1965–1985) (NUREG/CR-4945). U.S. Nuclear Regulatory Commission.

Mesarovic, M. D., Macko, D., and Takahara, Y. (1970). Theory of Hierarchical Multilevel Systems. Academic Press.

NEA/CSNI/R(2016)14 (2017, March). Scaling in System Thermal-Hydraulics Applications to Nuclear Reactor Safety and Design: A State-of-the-Art Report. Organisation for Economic Co-operation and Development, Nuclear Energy Agency.

Ransom, V. H., Wang, W., and Ishii, M. (1998). "Use of an Ideal Scaled Model for Scaling Evaluation." Nuclear Engineering and Design, 186, 135–147.

Reeder, D. L. (1980, September). LOFT System and Test Description (5.5 Foot Nuclear Core LOCEs) (NUREG/CR-0247, TREE-1208, Change 1). U.S. Nuclear Regulatory Commission.

Regulatory Guide 1.203 (2005, December). Transient and Accident Analysis Methods. U.S. Nuclear Regulatory Commission.

Reyes, J. N., Jr., and Hochreiter, L. (1998). "Scaling Analysis for the OSU AP600 Test Facility (APEX)." Nuclear Engineering and Design, 186, 53–109.

Schlesinger, S., Crosbie, R. E., Gagne, R. E., Innis, G. S., Lalwani, C. S., Loch, J., Sylvester, R. J., Wright, R. D., Kheir, N., and Bartos, D. (1979). "Terminology for Model Credibility." Simulation, 32(3), 103–104.

Vaschy, A. (1892). "*Sur les lois de similitude en physique*." *Annales Télégraphiques,* 19, 25–28.

Woodcock, J., and Dzodzo, M. B. (2000, April). "Application of Large Scale Containment Database to AP600 Loss-of-Coolant-Accident Internal Circulation and Stratification Evaluations." Proceedings of the 8th International Conference on Nuclear Engineering (ICONE-8466), Baltimore, MD.

Wulff, W., and Rohatgi, U. S. (1998, January). System Scaling for the Westinghouse AP600 Pressurized Water Reactor and Related Test Facilities: Analysis and Results (NUREG/CR-5541). U.S. Nuclear Regulatory Commission.

Wulff, W., Zuber, N., Rohatgi, U. S., and Catton, I. (2009). "Application of Fractional Scaling Analysis to Loss of Coolant Accidents, System Level Scaling for System Depressurization." *Journal of Fluids Engineering of The ASME*, 131, Article 081402.

Zuber, N. (1991, November). "A Hierarchical, Two-Tired Scaling Analysis." An Integrated Structure and Scaling Methodology for Severe Accident Technical Issue Resolution (NUREG/CR-5809, Appendix D). U. S. Nuclear Regulatory Commission.

Zuber, N., Rohatgi, U. S., Wulff, W., and Catton, I. (2007). "Application of Fractional Scaling Analysis (FSA) to Loss of Coolant Accidents (LOCA) Methodology Development." Nuclear Engineering and Design, 237, 1593–1607. https://doi:10.1016/j.nucengdes.2007.01.017

Zuber, N., Wilson, G. E., Ishii, M., Wulff, W., Boyack, B. E., Dukler, A. E., Griffith, P., Healzer, J. M., Henry, R. E., Lehner, J. R., et al. (1998). "An Integrated Structure and Scaling Methodology for Severe Accident Technical Issue Resolution: Development of Methodology." Nuclear Engineering and Design, 186, 1–21.

NONMANDATORY APPENDIX A
EXAMPLES OF EQUATIONS AND DIMENSIONLESS GROUPS USED FOR SCALING ANALYSIS

A-1 THE DIMENSIONLESS GROUPS IN H2TS

A-1.1 Example 1 — Surface and Volume Effects

(a) The dimensionless groups in H2TS (Zuber, 1991) can be represented by the ratio of surface effects (influences) to volumetric flow rate effects (influences) on the state variable (quantity of interest) change as shown in eq. (A-1-1) and Figure A-1.1-1:

$$\Pi = \frac{j \times A_T}{\psi \times \dot{V}} = \frac{j \times A_T}{\psi \times V_{\mathrm{CV}}} \times \frac{V_{\mathrm{CV}}}{\dot{V}} = \omega \times \tau \tag{A-1-1}$$

where the following definitions apply:

(1) The surface effects are represented by $j \times A_T$, which is the flux acting at the transfer area multiplied by the transfer area.

(2) The volume effects are presented by $\psi \times \dot{V}$, which is the product of the state variable, ψ, per unit of volume inside the control volume, V_{CV}, and the volumetric flow rate through the control volume.

(3) The characteristic time ratio Π represents a total change ratio of $\psi \times V$ (state variable ψ per volume inside the control volume V_{CV} multiplied by the control volume V_{CV}).

(4) $\omega = \frac{j \times A_T}{\psi \times V_{\mathrm{CV}}} = \omega_{A_T}$ represents the frequency of the state variable $\psi \times V_{\mathrm{CV}}$ change due to the surface transfer effects ω_{AT}.

(5) $\tau = \frac{V_{\mathrm{CV}}}{\dot{V}}$ represents the residence time inside the control volume V_{CV}.

The increase of the flux j and transfer area A_T surface (compared to the total control volume surface) will result in an increase of the frequency ω and time ratio Π. Also, the decrease of volumetric flow rate $\dot{V}$ through the control volume V_{CV} will result in an increase of the residence time τ and time ratio Π.

(b) The reciprocal value of the residence time $\frac{1}{\tau} = \frac{V_{\mathrm{CV}}}{\dot{V}} = \omega_{\dot{V}}$ is the frequency of the volume replacement and represents the frequency due to the convection (volumetric flow) effects. Thus, the dimensionless groups in H2TS can be also represented by the ratio of surface effects (influences) frequencies to volumetric flow rate effects (influences) frequencies on the state variable (quantity of interest) change:

$$\Pi = \frac{j \times A_T}{\psi \times \dot{V}} = \frac{j \times A_T}{\psi \times V_{\mathrm{CV}}} \times \frac{V_{\mathrm{CV}}}{\dot{V}} = \omega_{A_T} \times \tau = \frac{\omega_{A_T}}{\omega_{\dot{V}}} \tag{A-1-2}$$

The step-by-step derivation of H2TS dimensionless groups is presented in Table A-1.1-1.

(c) Sometimes the effects on the state variable can be volumetric. For example, there can be a volumetric heat source in the reactor vessel due to neutronic heating or buoyancy effects. In these cases, the dimensionless groups in H2TS can be represented by the ratio of effects (influences) inside the control volume to volumetric flow rate effects (influences) on the state variable (quantity of interest) change as shown in eq. (A-1-3):

$$\Pi = \frac{j_{\mathrm{CV}} \times V_{\mathrm{CV}}}{\psi \times \dot{V}} = \frac{j_{\mathrm{CV}} \times V_{\mathrm{CV}}}{\psi \times V_{\mathrm{CV}}} \times \frac{V_{\mathrm{CV}}}{\dot{V}} = \omega_{\mathrm{CV}} \times \tau = \frac{\omega_{\mathrm{CV}}}{\omega_{\dot{V}}} \tag{A-1-3}$$

where the following definitions apply:

(1) The volumetric effects are represented by $j_{\mathrm{CV}} \times V_{\mathrm{CV}}$, which is the volumetric source (or sink) acting at the control volume multiplied by the control volume.

Figure A-1.1-1
Control Volume, Transfer Area, Surface and Volume Effects, and State Variable

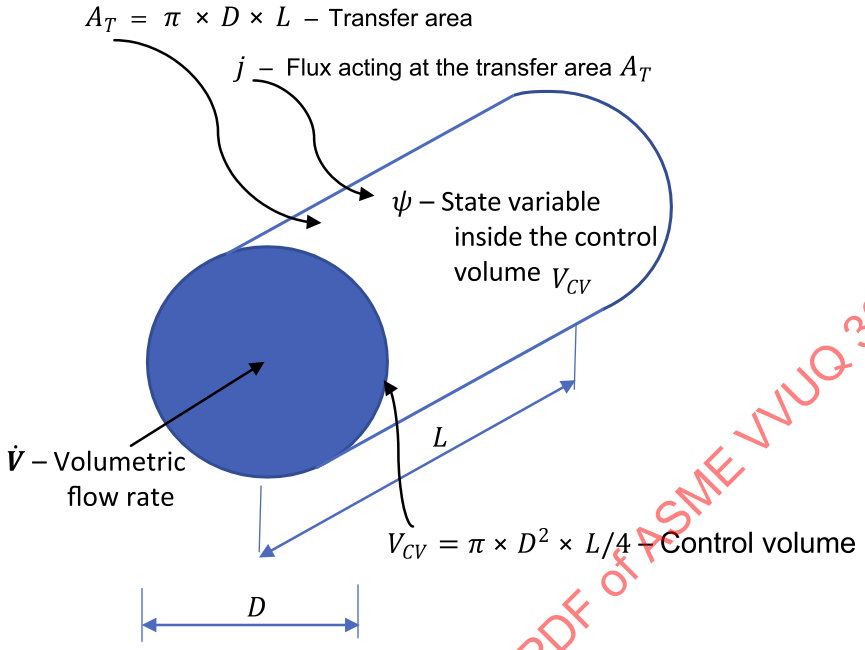

Table A-1.1-1
Examples of Derivations of H2TS Dimensionless Groups (Time Ratios)

Variables	Example 1	Example 2	Example 3
Characteristic length	$L = D$	$L = \frac{D}{4} = \frac{R}{2}$	...
Control volume	V_{CV}	$V_{\mathrm{CV}} = \pi R^2 \frac{R}{2}$	$V_{\mathrm{CV}} = \pi \times \left(\frac{L^2}{4}\right) \times L$
Transfer area	A_T	$A_{\mathrm{wall}} = 2\pi R \frac{R}{2}$	$A_T = \pi \times L \times L$
Surface effect	j	$\sigma_w = 2\mu v_{\max}/R$	$q'' = h_c \times (T_s - T_b)$
Volumetric flow rate	$\dot{V}$	$\dot{V} = v_{\max}\pi R^2/2$	$\dot{V} = \bar{v} \times \pi \times L^2/4$
State variable per volume	$\psi = \Psi/V_{\mathrm{CV}}$	Momentum $\psi = \rho \times \bar{v}$	Enthalpy $\psi = \rho \times c_p \times T_b = \rho \times h$
Frequency of change due to the surface transfer effects	$\omega_{A_T} = \frac{j \times A_T}{\psi \times V_{\mathrm{CV}}}$	$\omega_{A_T} = \omega_m = \frac{8 \times \nu}{R^2}$	$\omega_{A_T} = \frac{q'' \times A_T}{\rho \times h \times V_{\mathrm{CV}}}$
Residence time	$\tau = \frac{V_{\mathrm{CV}}}{\dot{V}}$	$\tau = \frac{R}{2 \times \bar{v}}$	$\tau = \frac{V_{\mathrm{CV}}}{\dot{V}}$
Frequency of the volume replacement due to the convection (volumetric flow) effects	$\omega_{\dot{V}} = 1/\tau = \dot{V}/V_{\mathrm{CV}}$	$\omega_{\dot{V}} = \frac{1}{\tau} = 2 \times \bar{v}/R$	$\omega_{\dot{V}} = 1/\tau = \dot{V}/V_{\mathrm{CV}}$
Time ratio	$\Pi = \frac{j \times A_T}{\psi \times \dot{V}} = \omega_{A_T} \times \tau = \frac{\omega_{A_T}}{\omega_{\dot{V}}}$	$\Pi_{Re} = \frac{8 \times \nu}{R^2} \times \frac{\frac{R}{2}}{\bar{v}} = \frac{2 \times \nu}{L^2} \times \frac{L}{\bar{v}} = \omega_m \tau \sim \frac{\nu}{L \times \bar{v}} = \frac{1}{Re}$	$\Pi = \frac{q'' \times A_T}{\rho \times h \times V_{\mathrm{CV}}} \times \frac{V_{\mathrm{CV}}}{\dot{V}} = \omega_{A_T} \times \tau = \frac{\omega_{A_T}}{\omega_{\dot{V}}}$

(2) The volume effects are presented by $\psi \times \dot{\boldsymbol{V}}$, which is the product of the state variable ψ per unit of volume inside the control volume V_{CV} and the volumetric flow rate through the control volume.

(3) The characteristic time ratio Π represents a total change ratio of $\psi \times V_{CV}$ (state variable ψ per volume inside the control volume V_{CV} multiplied by the control volume V_{CV}).

(4) $\omega = \dfrac{j_{CV} \times V_{CV}}{\psi \times V_{CV}} = \omega_{CV}$ represents the frequency of the state variable $\psi \times V_{CV}$ change due to the volumetric sources (or sinks) effects ω_{CV}.

(5) $\tau = \dfrac{V_{CV}}{\dot{\boldsymbol{V}}}$ represents the residence time inside the control volume V_{CV}.

(6) $\omega_{\dot{\boldsymbol{V}}}$ is the frequency of the volume replacement and represents the frequency due to the convection (volumetric flow) effects.

A-1.2 Example 2 — The Time–Ratio Relation to the Reynolds Number

The time–ratio relation to the Reynolds number can be established with the H2TS approach as shown in eq. (A-1-2):

$$\begin{aligned} \Pi_{Re} &= \frac{j \times A_T}{\psi \times \dot{\boldsymbol{V}}} = \frac{j \times A_T}{\psi \times V_{CV}} \frac{V_{CV}}{\dot{\boldsymbol{V}}} \\ &= \frac{\sigma_{wall} \times A_{wall}}{\rho \times \bar{v} \times V_{CV}} \frac{V_{CV}}{\dot{\boldsymbol{V}}} \end{aligned} \tag{A-1-4}$$

A_{wall} = wall surface
$\bar{v}$ = average velocity
ρ = density
σ_{wall} = wall shear stress

Based on the solution for the laminar fully developed pipe flow velocity profile $v = v_{max}(1 - r^2/R^2)$, with pipe radius R and maximum velocity in the pipe center v_{max}, the following terms in eq. (A-1-4) can be calculated:

(a) volumetric flow $\dot{\boldsymbol{V}} = v_{max}\pi R^2/2$

(b) average velocity $\bar{v} = \dot{\boldsymbol{V}}/A = \dot{\boldsymbol{V}}/\left(\pi R^2\right) = v_{max}/2$

(c) wall shear $\sigma_w = |\mu(dv/dr)|_{r=R} = 2\mu v_{max}/R$

Based on the spatial scale $L = D/4 = R/2$ defined by the transfer area concentration $1/L = A_w/V_{CV} = 4/D = 2/R$, as in Zuber et al., 2007, equation (A-1-4) can be rearranged as follows:

$$\begin{aligned} \Pi_{Re} &= \frac{\sigma_{wall}}{\rho \times \bar{v}} \times \frac{A_{wall}}{V_{CV}} \times \frac{V_{CV}}{\dot{\boldsymbol{V}}} \\ &= \frac{\frac{2\mu v_{max}}{R}}{\rho \frac{v_{max}}{2}} \times \frac{2\pi R \frac{R}{2}}{\pi R^2 \frac{R}{2}} \times \frac{\pi R^2 \frac{R}{2}}{\bar{v}\pi R^2} = \frac{8 \times \nu}{R^2} \times \frac{\frac{R}{2}}{\bar{v}} \\ &= \frac{2 \times \nu}{L^2} \times \frac{L}{\bar{v}} = \omega_m \tau \sim \frac{\nu}{L \times \bar{v}} = \frac{1}{\mathrm{Re}} \end{aligned} \tag{A-1-5}$$

where
μ = dynamic fluid viscosity
ν = kinematic fluid viscosity

In eq. (A-1-5), the frequency $\omega_m = \dfrac{2 \times \nu}{L^2}$ represents the temporal scale for the diffusion process (Zuber et al., 2007) and the residence time $\tau = \dfrac{V_{CV}}{\dot{\boldsymbol{V}}} = \dfrac{A \times L}{A \times \bar{v}} = \dfrac{L}{\bar{v}}$ represents the temporal scale for the convection process.

A-1.3 Example 3 — The Power-to-Volume Scaling Criterion

Another example, similar to the one presented in Zuber et al. (1998), is the dimensional group for heat transfer to a fluid flowing inside a pipe. The heat flux is represented by

$$j = q'' = h_c \times (T_s - T_b) \tag{A-1-6}$$

where

h_c = convective heat transfer coefficient
T_b = fluid bulk temperature
T_s = wall surface

The pipe is of length L, and diameter $D = L$. Thus, the heat transfer area is represented by

$$A_T = \pi \times L \times D = \pi \times L \times L \tag{A-1-7}$$

And the control volume is represented by

$$V_{\mathrm{CV}} = \pi \times \left(\frac{D^2}{4}\right) \times L = \pi \times \left(\frac{L^2}{4}\right) \times L \tag{A-1-8}$$

Using an average velocity, $\bar{v}$, the volumetric flow rate is represented by

$$\dot{\boldsymbol{V}} = \bar{v} \times \pi \times L^2/4 \tag{A-1-9}$$

The characteristic time ratio can then be formulated as shown in eq. (A-1-10):

$$\Pi = \frac{j \times A_T}{\psi \times \dot{\boldsymbol{V}}} = \frac{[h_c \times (T_s - T_b)] \times [\pi \times L \times L]}{\left[\rho \times c_p \times T_b\right] \times \left[\bar{v} \times \pi \times L^2/4\right]} = \frac{q'' \times A_T}{\rho \times h \times V_{\mathrm{CV}}} \times \frac{V_{\mathrm{CV}}}{\dot{\boldsymbol{V}}} = \omega \times \tau \tag{A-1-10}$$

The characteristic frequency ω specifies how many times per second the enthalpy contained in the expression $\rho \times h \times V_{\mathrm{CV}}$ is being changed due to a heat transfer at the pipe surface $q" \times A_T$ (transfer process). The characteristic time ratio Π is the total change ratio during the residence time $\tau = V_{\mathrm{CV}}/\dot{\boldsymbol{V}}$.

The power-to-volume scaling criterion [see eq. (3-1-1), repeated below] can be derived from eq. (A-1-10) if the IET facility (model) operates at prototypical pressure with the same fluid ($\rho_M = \rho_P$) and ($h_{\mathrm{Model}} = h_{\mathrm{Prototype}}$) and residence times ($\tau_{Model} = \tau_{Prototype} = \frac{V_{\mathrm{CV}}}{\dot{\boldsymbol{V}}}$) as in NPP (prototype).

$$[q'' \times A_T/V_{\mathrm{CV}}]_M = [q'' \times A_T/V_{\mathrm{CV}}]_P$$

A-2 THE DIMENSIONLESS GROUPS IN FSA

To quantify the effect of a change in state variable (quantity of interest) Ψ in control volume by an amount $\delta\Psi$, the reference value Ψ_0 can be used to define fractional change (effect metric), Ω, as follows:

$$\Omega = \frac{\delta\Psi}{\Psi_0} = \frac{\omega \times \Psi \times \delta t}{\Psi_0} = \frac{\Phi}{\Psi_0}\,\delta t \tag{A-2-1}$$

In eq. (A-2-1), ϕ is the agent of change (influence) causing certain change of a state variable (quantity of interest) Ψ per time and is represented by

$$\Phi = \frac{d\Psi}{dt} \tag{A-2-2}$$

Also, in eq. (A-2-1), ω, in units of 1/s, is the FRC of state variable Ψ and is represented by

$$\omega = \frac{\left(\frac{d\Psi}{dt}\right)}{\Psi} = \frac{\Phi}{\Psi} \tag{A-2-3}$$

For example, if the state variable is energy E (see Table A-2-1) in the unit of joules (J), the agent of change is power, P, and is equal to $\Phi = d\Psi/dt = dE/dt = P$ in the unit of watts (W). The FRC is equal to $\omega = (d\Psi/dt)/\Psi = \Phi/\Psi = P/E$ in the units of 1/s. The fractional change (effect metrics) is then equal to $\Omega = (P/E_0) \times \delta t$ in which E_0 is the reference value of energy.

The fractional change (effect metric) Ω, FRC ω, and agent of change Φ for several state variables are presented in Table A-2-1. As an illustration of how FSA might be used in other fields of science some variables of interest to biology and economy are specified in the last two columns of Table A-2-1.

Based on Zuber et al. (2007), the reciprocal value of residence time (or the volume turnover time) is the volume replacement frequency, which is the temporal scale for convection process in FSA.

$$\omega_\tau = \frac{1}{\tau} = \frac{\dot{V}}{A \times L} = \frac{A \times \bar{v}}{A \times L} = \frac{\bar{v}}{L} \tag{A-2-4}$$

The temporal scale for diffusion process (Zuber et al., 2007) can be expressed as a FRC where the state variable is momentum, $\Psi = m \times \bar{v}$, and the agent of change is the shear force, $\phi = F_w = \sigma_w \times A_w$, at the wall (see the "Momentum" column in Table A-2-1):

$$\begin{aligned} \omega_m = \frac{\Phi}{\Psi} &= \frac{F_w}{m \times \bar{v}} = \frac{\sigma_w \times A_w}{\rho \times A \times L \times \bar{v}} \\ &= \frac{2 \times \nu}{L^2} \sim \frac{\nu}{L^2} \end{aligned} \tag{A-2-5}$$

Based on the FSA approach, the Reynolds number can then be defined as the ratio of temporal scales for the convection and diffusion processes. The normalized fractional change (effect metric) Ω^+_{Re} is then

$$\Omega^+_{\mathrm{Re}} = \frac{\omega_\tau}{\omega_m} = \frac{\frac{\bar{v}}{L}}{\frac{2 \times \nu}{L^2}} \sim \frac{\frac{\bar{v}}{L}}{\frac{\nu}{L^2}} = \frac{\bar{v} \times L}{\nu} = \mathrm{Re} \tag{A-2-6}$$

In the case that multiple n agents of change ϕ_j (where j = 1 to n) are present, the normalized fractional change (effect metric) Ω^+_j can be obtained from

$$\begin{aligned} \Omega^+_j &= \frac{\Omega_j}{|\Omega_1 + \Omega_2 + \cdots + \Omega_n|} \\ &= \frac{\omega_j}{|\omega_1 + \omega_2 + \cdots + \omega_n|} = \frac{\omega_j}{|\bar{\omega}|} \end{aligned} \tag{A-2-7}$$

in which $\bar{\omega}$ is the effective FRC, in units of 1/s.

Table A-2-1 is applied in section A-3 for a reactor pressure response, section A-4 for reactor vessel water level response, and section A-5 on peak cladding temperature.

Table A-2-1
State Variables, Agents of Change, FRCs, and Fractional Changes (Effect Metrics)

State Variable, Ψ	Volume, V	Mass, m	Momentum, $m\bar{v}$	Energy, E	Ecology/ Biology	Economy
Agent of change $\Phi = \frac{d\Psi}{dt}$	Volumetric dilatation $\Phi = \frac{dV}{dt} = \dot{V}$	Mass flow rate $\Phi = \frac{dm}{dt} = \dot{m}$	Force $\Phi = \frac{d(m\bar{v})}{dt} = F$	Power $\phi = \frac{dE}{dt} = P$	Population/ biomass	Capital
FRC $\omega = \frac{\left(\frac{d\Psi}{dt}\right)}{\Psi} = \frac{\Phi}{\Psi}$	Volumetric dilatation rate $\omega = \frac{(\dot{V})}{V}$	$\omega = \frac{\dot{m}}{m}$	Mechanical impedance $\omega = \frac{F}{m\bar{v}}$	$\omega = \frac{P}{E}$	Reproductive force	Economic force
Fractional change/ effect metrics $\Omega = \frac{\delta\Psi}{\Psi_0} = \frac{\omega \times \Psi \times \delta t}{\Psi_0} = \frac{\Phi}{\Psi_0}\delta t$	$\Omega = \frac{\left(\frac{dV}{dt}\right)}{V_0}\delta t$	$\Omega = \frac{\dot{m}}{m_0}\delta t$	$\Omega = \frac{F}{(m\bar{v})_0}\delta t$	$\Omega = \frac{P}{E_0}\delta t$	Specific growth rate	Interest rate

GENERAL NOTE: The table is reprinted from *Nuclear Engineering and Design*, 237, Zuber, N., Rohatgi, U. S., Wulff, W., and Catton, I., "Application of Fractional Scaling Analysis (FSA) to Loss of Coolant Accidents (LOCA) Methodology Development," 1593–1607, 2007, with permission from Elsevier.

A-3 REACTOR VESSEL PRESSURE RESPONSE

The pressure response equation might be derived by combining the total mass and energy balances in a system control volume V (see Figure 5.2-1). The system control volume might be occupied by any combination of subvolumes, subcooled single-phase liquid $V_{1\phi l}$, single-phase vapor $V_{1\phi v}$, saturated two-phase mixture $V_{2\phi}$, and noncondensable nitrogen gas V_{N2}, where $V = V_{1\phi l} + V_{1\phi v} + V_{2\phi} + V_{N_2}$.

The form of pressure response equation, eq. (A-3-1) derived in Wulff and Rohatgi (1998) and presented in Wulff et al. (2009), is used for this analysis. The assumptions and details of the derivation of the equation are available in Wulff and Rohatgi. This form of equation is suitable for FSA because each term in the equation represents the influence of one phenomenon (i.e., agent of change) affecting the pressure response:

$$\dot{p} = \frac{1}{VK_{s,\mathrm{sys}}}\left[\sum_{j=bk,\mathrm{ADS}} \dot{V}_j + \frac{v_{fg}}{h_{fg}}\dot{Q}_{2\varnothing} + \sum_{j=1\varnothing l,1\varnothing v}\left(\frac{\beta_T}{\rho c_p}\dot{Q}\right)_j + \left(\frac{\beta_T}{\rho c_p}\right)_l P_{\mathrm{pp}} + \frac{\gamma-1}{\gamma}\frac{\dot{Q}_{N_2}}{p}\right] \tag{A-3-1}$$

In eq. (A-3-1), each of the following terms in the square bracket is a rate of volume change:

(a) the sum of volumetric flow rates $\sum_{j=bk,\mathrm{ADS}} \dot{V}_j$ leaving ($\dot{V}_j < 0$), or entering ($\dot{V}_j > 0$) the control volume V through the break and valve openings

(b) the rate of expansion or contraction due to the heating or cooling rate of phase change $\dot{Q}_{2\varnothing}$

(c) the rates of volumes change due to thermal expansion or contraction by net heating or cooling rate, $\dot{Q}_{\mathrm{net}}$ in single-phase regions (like subcooled liquid $\dot{Q}_{1\varnothing,l}$, or vapor $\dot{Q}_{1\varnothing,v}$)

(d) the rate of volume change due to thermal expansion by adding pumping power P_{PP} in single-phase region of subcooled liquid l

(e) the rate of volume changes due to the inert gas rate of heating or cooling $\dot{Q}_{N_2}$

In eq. (A-3-1), the denominator $VK_{s,sys}$ is the total system elasticity or "mechanical compliance", in which the system isentropic compressibility $K_{s,\mathrm{sys}}$ is calculated as the volume fraction-weighted average of the isentropic compressibility, $\kappa_s = c_v\kappa/c_p$ (where $\kappa = (\partial\rho/\partial p)_T/\rho$ represents the isothermal compressibility), related to each subvolume V_i of the control volume V presented in Figure 5.4-1.

$$K_{s,\mathrm{sys}} = \sum_{i=l,v,2\phi,N_2} K_{s,\mathrm{sys}_i} = \sum_{i=l,v,2\phi,N_2} \frac{V_i}{V}(\kappa_s)_i \tag{A-3-2}$$

The summation of isentropic compressibility for each subvolume produces

$$K_{s,\mathrm{sys}} = \sum_{j=l,v}\left(\frac{c_v\kappa}{c_p}\right)_j\frac{V_j}{V} + \left\{\sum_{k=g,f}\alpha_k\left[\frac{v_{fg}}{h_{fg}}(\rho_k h_k' - 1) + \frac{\rho_k'}{\rho_k}\right]\right\}\frac{V_{2\phi}}{V} + \frac{1}{\gamma p}\frac{V_{N_2}}{V} \tag{A-3-3}$$

The terms with primes in the expression of the isentropic compressibility for two-phase mixture, represent density and enthalpy derivatives with respect to pressure along the saturation line from Wulff et al. (2009) as follows:

$$\rho_k' = \frac{1}{\rho_k} + \left[1 - T_{\mathrm{sat}}\frac{v_{fg}}{h_{fg}}\left(\frac{\partial p}{\partial T}\right)_{\rho_k}\right], \quad k = g, f \tag{A-3-4}$$

$$h_k' = \frac{1}{\rho_k} + T_{\mathrm{sat}}\left[(c_p)_k\frac{v_{fg}}{h_{fg}} - \frac{\beta_k}{\rho_k}\right], \quad k = g, f \tag{A-3-5}$$

Table A-3-1 shows the dimensionless agents of change and fractional rates of change for terms in eq. (A-3-1).

Figure A-3-1 shows the pressurized water reactor (PWR) vessel pressure responses in dimensional form according to eq. (A-1-1) for pressure as a function of time. These pressure responses were taken for LOFT and Semiscale facilities at different percentages of SBLOCA.

Table A-3-1
Definition of Dimensionless Agents of Change and Fractional Rates of Change for Pressure Response Equation

Description of Agents of Change System or Boundary Effects	Dimensionless Agents of Change, Φ_j^+	Initial Fractional Rates of Change, ω_j
Break flow, inlet and outlet j = 1	$\Phi_{bk}^+ = \dfrac{\dot{V}_{bk}^+}{K_{s,\mathrm{sys}}^+}$	$\omega_{bk} = \dfrac{(\dot{V}_{bk})_0}{V\Delta p_0 \left(K_{s,\mathrm{sys}}\right)_0}$
Phase change by heating/cooling j = 2	$\Phi_{\dot{Q}_{2\varnothing}}^+ = \dfrac{\left(v_{fg}/h_{fg}\right)^+}{K_{s,\mathrm{sys}}^+}\left(\dot{Q}_{2\varnothing}\right)_{\mathrm{net}}^+$	$\omega_{\dot{Q}_{2\varnothing}} = \dfrac{\left(v_{fg}/h_{fg}\right)_0\left(\dot{Q}_{2\varnothing}\right)_{net,0}}{V\Delta p\left(K_{s,\mathrm{sys}}\right)_0}$
Single phase thermal expansion/contraction by heating/cooling j = l, v = 3, 4	$\Phi_{\dot{Q}_{1\varnothing}}^+ = \dfrac{\left[\beta/\left(\rho\times c_p\right)\right]_{1\phi}^+}{K_{s,\mathrm{sys}}^+}\left(\dot{Q}_{1\varnothing}\right)_{\mathrm{net}}^+$	$\omega_{\dot{Q}_{1\varnothing}} = \dfrac{\left[\beta/\left(\rho\times c_p\right)\right]_{1\varnothing,0}\left(\dot{Q}_{1\varnothing}\right)_{\mathrm{net},0}}{V\Delta p\left(K_{s,\mathrm{sys}}\right)_0}$
Expansion due to the heating by recirculation pumps j = 5	$\Phi_{\mathrm{PP}}^+ = \dfrac{\left[\beta/\left(\rho\times c_p\right)\right]_l^+}{K_{s,\mathrm{sys}}^+}P_{\mathrm{PP}}^+$	$\omega_{\mathrm{PP}} = \dfrac{\left[\beta/\left(\rho\times c_p\right)\right]_{l,0}(P_{\mathrm{PP}})_0}{V\Delta p\left(K_{s,\mathrm{sys}}\right)_0}$
Expansion/contraction of inert gas due to heating/cooling j = 6	$\Phi_{\dot{Q}_{N_2}}^+ = \dfrac{1}{K_{s,\mathrm{sys}}^+(p^+ + p_{\min}/\Delta p)}\dot{Q}_{N_2}^+$	$\omega_{\dot{Q}_{N_2}} = \dfrac{\gamma-1}{\gamma}\dfrac{\left(\dot{Q}_{N_2}\right)_0}{V\left(\Delta p_0 \times p_0\right)\left(K_{s,\mathrm{sys}}\right)_0}$

GENERAL NOTE: The table is based on Wulff et al. (2009) with permission from the *Journal of Fluids Engineering*.

By applying Table A-3-1, the pressure response eq. (A-3-1) can be modified (normalized) and presented in dimensionless form as follows:

$$\frac{dp^+}{dt} = \omega_{bk}\Phi_{bk}^+ + \omega_{2\phi}\Phi_{2\phi}^+ + \omega_l\Phi_l^+ + \omega_g\Phi_g^+ + \omega_{PP}\Phi_{PP}^+ + \omega_{N_2}\Phi_{N_2}^+ \tag{A-3-6}$$

or

$$\frac{dp^+}{dt^+} \equiv \sum_{j\,=\,1,6}\frac{\omega_j}{|\overline{\omega}|}\Phi_j^+ \tag{A-3-7}$$

where

t^+ = dimensionless time
= $|\overline{\omega}| \times t$
$|\overline{\omega}|$ = effective FRC of the system
= $\left|\Sigma_{j\,=\,1,n}\,\omega_j\right|$

Figure A-3-2 shows the PWR vessel pressure responses in dimensionless form according to eq. (A-3-7) for fractional pressure as a function of fractional change metric. These pressure responses were taken for LOFT and Semiscale facilities at different percentages of SBLOCA.

The FRCs ω_j and dimensionless agents of change Φ_j^+ in eq. (A-3-7) are specified in Table A-3-1.

It should be noted that the reference quantities used in nondimensionalizing variables for each time sequence of the transient should be validated with the available data if the tests have been performed.

The test results for various test facilities (see Figure A-3-1) are in agreement if all results are presented in dimensionless form (see Figure A-3-2) as in eq. (A-3-7). The agreement is reached when all test facilities (presented in Figure 3.2-1) are designed (scaled) to simulate the same PWR design and the relative simple start of an accident when the break effects are dominant.

Figure A-3-1
PWR Vessel Pressure Responses for Various Test Facilities in Dimensional Form

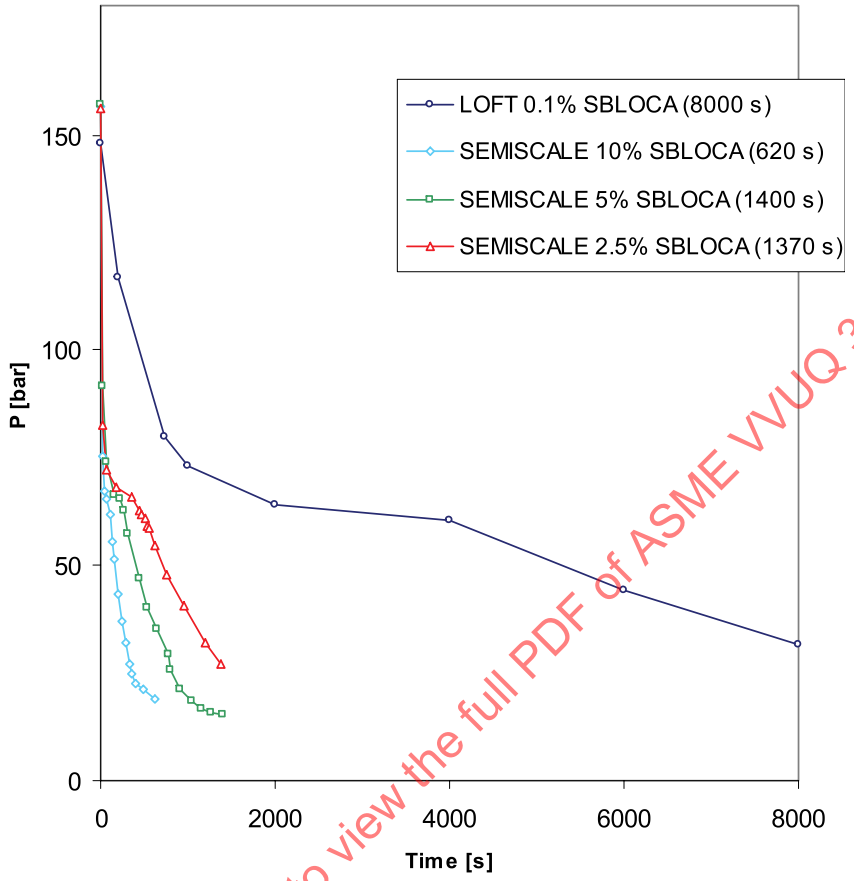

Figure A-3-2
PWR Vessel Pressure Responses for Various Test Facilities in Dimensionless Form

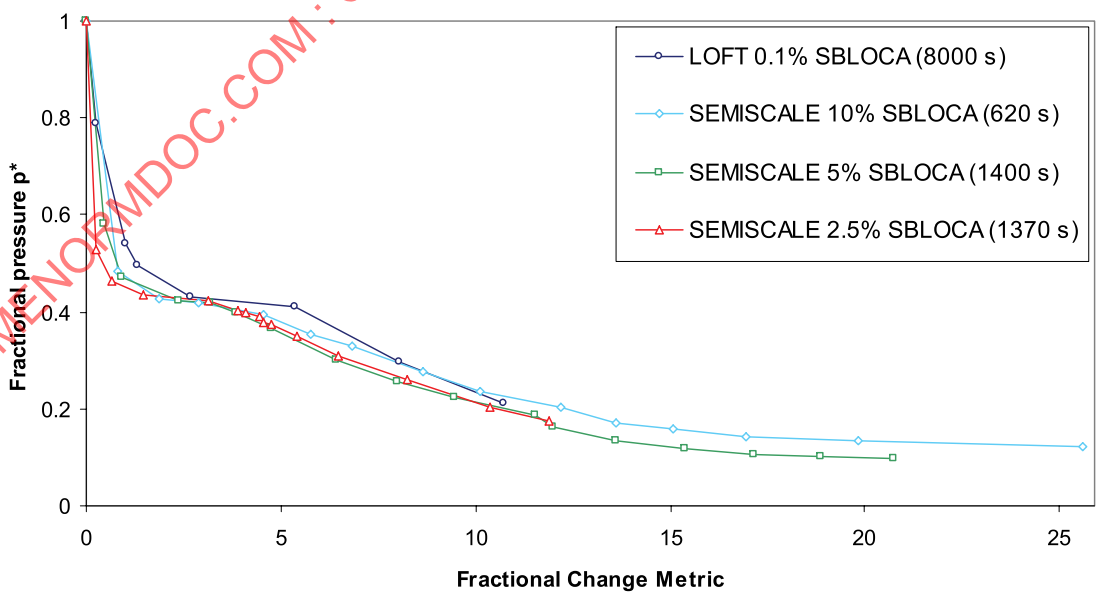

A-4 REACTOR VESSEL WATER LEVEL RESPONSE

The void fraction of the entire reactor vessels can be used for the scaling analysis for the void fraction equation (in fact, the total reactor vessel volume V is considered as two-phase mixture volume $V_{2\phi}$, $V = V_{2\phi}$). The equation for void fraction derived as in Wulff and Rohatgi (1998) can be applied for the analysis as follows:

$$\frac{d\alpha}{dt} = \frac{\dot{V}_{g,\text{in}} - \dot{V}_{g,\text{out}}}{V} + \dot{Q}_{2\varnothing}\left(\frac{1}{\rho_g h_{fg} V}\right) - \dot{p}\Psi_\alpha \tag{A-4-1}$$

Substituting the time derivative of pressure, $\dot{p}$ in eq. (A-3-1), into the last term of eq. (A-4-1), eq. (A-4-1) can be re-written as follows:

$$\begin{aligned}\frac{d\alpha}{dt} = {} & \frac{\dot{V}_{g,\text{in}} - \dot{V}_{g,\text{out}}}{V} + \dot{Q}_{2\varnothing}\left(\frac{1}{\rho_g h_{fg} V}\right) - \frac{\Psi_\alpha}{VK_{s,\text{sys}}}\left[-\sum\nolimits_{j=bk,\text{ADS}} \dot{V}_j + \frac{v_{\text{fg}}}{h_{\text{fg}}}\left(\dot{Q}_{2\varnothing}\right)_{\text{net}}\right. \\ & \left. + \sum\nolimits_{j=1\varnothing l,1\varnothing v}\left(\frac{\beta_T}{\rho c_p}\dot{Q}\right)_j + \left(\frac{\beta_T}{\rho c_p}\right)_l P_{pp} + \frac{\gamma-1}{\gamma}\frac{\dot{Q}_{N_2}}{p}\right]\end{aligned} \tag{A-4-2}$$

The multiplier of $\dot{p}$ in the last term of eqs. (A-4-1) and (A-4-2) is as follows:

$$\Psi_\alpha = \frac{\alpha\left(\rho_g' h_{fg} + \rho_g h_g'\right) + (1-\alpha)\rho_l h_l' - 1}{\rho_g h_{fg}} \tag{A-4-3}$$

To obtain the fractional rates of change and agents of change for void fraction, eq. (A-4-2) can be normalized in a similar way as the pressure response equation in section A-1. Equation (A-4-4) is obtained after normalization as follows:

$$\begin{aligned}\frac{d\alpha^+}{dt} = {} & \frac{\left(\dot{V}_{g,\text{in}} - \dot{V}_{g,\text{out}}\right)_0}{V}\frac{\dot{V}_{g,\text{in}} - \dot{V}_{g,\text{out}}}{\left(\dot{V}_{g,\text{in}} - \dot{V}_{g,\text{out}}\right)_0} + \frac{\left(\dot{Q}_{2\varnothing}\right)_0}{V\left(\rho_g h_{fg}\right)_0}\frac{\frac{\dot{Q}_{2\varnothing}}{\left(\dot{Q}_{2\varnothing}\right)_0}}{\frac{\rho_g h_{fg}}{\left(\rho_g h_{fg}\right)_0}} \\ & + \frac{\left(\sum_{j=bk,\text{ADS}} \dot{V}_j\right)_0 (\Psi_\alpha)_0}{V\left(K_{s,\text{sys}}\right)_0}\frac{1}{\frac{K_{s,\text{sys}}}{\left(K_{s,\text{sys}}\right)_0}}\frac{\sum_{j=bk,\text{ADS}} \dot{V}_j}{\left(\sum_{j=bk,\text{ADS}} \dot{V}_j\right)_0}\frac{\Psi_\alpha}{(\Psi_\alpha)_0} \\ & - \frac{\left(\frac{v_{fg}}{h_{fg}}\right)_0 \left(\dot{Q}_{2\varnothing}\right)_{\text{net},0} (\Psi_\alpha)_0}{V\left(K_{s,\text{sys}}\right)_0}\frac{1}{\frac{K_{s,\text{sys}}}{\left(K_{s,\text{sys}}\right)_0}}\frac{\frac{v_{fg}}{h_{fg}}\left(\dot{Q}_{2\varnothing}\right)_{\text{net}}}{\left(\frac{v_{fg}}{h_{fg}}\right)_0 \left(\dot{Q}_{2\varnothing}\right)_{\text{net},0}}\frac{\Psi_\alpha}{(\Psi_\alpha)_0} - \cdots\end{aligned} \tag{A-4-4}$$

Note that $\alpha = \alpha^+$ is already a dimensionless variable. After normalization the equation takes the following form:

$$\begin{aligned}\frac{d\alpha^+}{dt} = {} & \omega_{\dot{V}_g}\Phi^+_{\dot{V}_{g,in}} + \omega_{\dot{Q}_{2\varnothing}}\Phi^+_{\dot{Q}_{2\varnothing}} + \omega_{bk,\text{ADS},\dot{p}}\Phi^+_{bk,\text{ADS},\dot{p}} + \omega_{\dot{Q}_{2\varnothing},\dot{p}}\Phi^+_{\dot{Q}_{2\varnothing},\dot{p}} + \omega_{\dot{Q}_l,\dot{p}}\Phi^+_{\dot{Q}_l,\dot{p}} + \omega_{\dot{Q}_v,\dot{p}}\Phi^+_{\dot{Q}_v,\dot{p}} \\ & + \omega_{PP,\dot{p}}\Phi^+_{PP,\dot{p}} + \omega_{\dot{Q}_{N_2},\dot{p}}\Phi^+_{\dot{Q}_{N_2},\dot{p}}\end{aligned} \tag{A-4-5}$$

The fractional rates of change and agent of change in eq. (A-4-4) are presented in Table A-4-1.

A-5 PEAK CLADDING TEMPERATURE

FSA is demonstrated in Catton et al. (2009) at the component level for depressurization of nuclear reactor primary systems undergoing a large break loss of coolant accident. FSA is used to estimate peak cladding temperature (PCT) as an example. This analysis is based on a fuel thermal analysis. The clad temperature, T_w, is affected by power (decay power),